LATERAL VIBRATIONS AS RELATED TO STRUCTURAL STABILITY

Thesis by

Harold Lurie

In Partial Fulfillment of the Requirements

For the Degree of

Doctor of Philosophy

California Institute of Technology

Pasadena, California

1950

ACKNOWLEDGMENTS

The author wishes to express his appreciation to Dr. E. E. Sechler for his ready advice and constant encouragement throughout the work. He is particularly indebted to Dr. G. W. Housner for suggesting the general problem, and to Dr. D. E. Hudson for his invaluable guidance and generous help.

ABSTRACT

The apparently different physical problems of lateral vibration and elastic stability are limiting cases of a single phenomenon, the most general expression being the mode of vibration with end thrust. The theory of straight beams and flat plates is discussed in detail, and it is shown that the square of the frequency of lateral vibration is approximately linearly related to the end load. The linear relationship is exact if the mode of free vibrations is identical to the buckling mode. In all cases, the load corresponding to zero frequency is the critical buckling load. The analysis is valid only if the boundary conditions do not change with load.

Experimental tests were conducted on elastically restrained columns in the form of rigid rectangular frames. It is found that the relationship between the square of the frequency and the load is practically linear, and that the extrapolated load corresponding to zero frequency coincides with the buckling load. Determining the critical load by frequency measurements seems to have the advantage of predicting that load corresponding to the actual boundary conditions which prevail, whereas a theoretical calculation may unjustifiably assume certain conditions which are not exactly realized.

In the case of flat plates, tests showed that the linear relationship is not achieved in practice. It is shown that this is probably due to the fact that the linear plate equations are not valid due

to initial curvatures in the plate.

Rigid-joint trusses were also tested. Due to the change of end restraint with load, in some cases the relationship between the square of the frequency and the load deviates considerably from linearity. The amount of deviation appears to depend on the section properties of the members of the truss.

TABLE OF CONTENTS

LIST OF FIGURES

LIST OF SYMBOLS

$\rho(x)$ = mass per unit length

$p(x)$ = transverse load per unit length

$u(x_i;t)$ = resultant deflection

$w(x)$ = synchronous deflection function for free vibrations

$v(x)$ = synchronous deflection function with end thrust

$g(t)$ = variation of deflection with time.

c^2 = $\frac{\rho}{EI}$

β^2 = $\frac{P}{EI}$

ω_n = frequency for free vibrations in $n^{\underline{th}}$ mode

ω^*_n = frequency for vibrations with end thrust in $n^{\underline{th}}$ mode

$2h$ = plate thickness

D = plate rigidity = $\frac{Eh^3}{12(1-\nu^2)}$

$q(x,y)$ = transverse load per unit area

$\mu(x,y)$ = mass per unit area

PART I

INTRODUCTION

Problems which relate either to the free vibrations or to the stability of elastic systems have received wide attention, and both phenomena have been investigated very thoroughly. It has long been recognized that there is in fact no real distinction between the two classes of problems; mathematically they are identical.

It is interesting to note that in addition to the similarity between the simple problem of free vibrations and of elastic stability, some very striking analogies occur when certain modifications are introduced. A good example is provided by considering forced vibrations and the stability of an initially curved member. To illustrate this, a uniform beam has been chosen for simplicity.

(a) Consider a uniform beam subjected to a load that is a harmonic function of time. The differential equation for the deflection y of a vibrating beam is given by

$$EI \frac{\partial^4 y}{\partial x^4} + \rho \frac{\partial^2 y}{\partial t^2} = 0$$

when there are no external forces. If the load per unit length is equal to $p(x) \sin \omega t$, the equation of motion becomes

$$EI \frac{\partial^4 y}{\partial x^4} + \rho \frac{\partial^2 y}{\partial t^2} = p(x) \sin \omega t$$

Separating variables, the solution can be written as

$$y = w(x) \sin \omega t$$

Therefore w(x) must satisfy the total differential equation

$$EI \frac{d^4 w}{dx^4} - \rho \omega^2 w = p(x)$$

If the beam is assumed to be hinged at each end and if $p(x) = p_o \sin \frac{\pi x}{\ell}$, then w(x) can be written as $w(x) = w_o \sin \frac{\pi x}{\ell}$. Substituting these values into the above differential equation,

$$w_o = \frac{p_o}{EI \frac{\pi^4}{\ell^4} - \rho \omega^2}$$

$$\text{or} \quad w_o = \frac{p_o \ell^4}{EI \pi^4} \cdot \frac{1}{1 - \frac{\rho \omega^2 \ell^4}{EI \pi^4}}$$

An examination of the terms in this expression reveals that (i) $\frac{p_o \ell^4}{EI \pi^4}$ is the coefficient for the deflection w(x) if p(x) is a stationary load, and (ii) $EI\pi^4/\rho\ell^4$ is the square of the fundamental frequency ω_o of the beam.

Hence the deflection curve for a forced vibration with frequency ω can be obtained by multiplying the static deflection curve by the "resonance factor" $\frac{1}{1 - (\frac{\omega}{\omega_o})^2}$.

(b) Consider a column under the action of an end thrust P, and which has an initial curvature given by

$$w = w_o \sin \frac{\pi x}{\ell}$$

If the column is assumed to be hinged at each end, then the equation governing the form of the strained central line is

$$EI\left(\frac{d^2y}{dx^2} - \frac{d^2w}{dx^2}\right) = -Py .$$

But $\frac{d^2w}{dx^2} = -\frac{w_0\pi^2}{\ell^2}\sin\frac{\pi x}{\ell}$,

$$\therefore \frac{d^2y}{dx^2} + \beta^2 y = -\frac{w_0\pi^2}{\ell^2}\sin\frac{\pi x}{\ell}$$

where $\beta^2 = \frac{P}{EI}$.

The solution of this differential equation is

$$y = A\cos\beta x + B\sin\beta x + \frac{w_0\pi^2}{\pi^2 - \beta^2\ell^2}\sin\frac{\pi x}{\ell} .$$

The boundary conditions are:

(i) y = 0 when x = 0

(ii) y = 0 when x = ℓ.

The first yields A = 0.

The second requires B $\sin\beta\ell = 0$,

i.e. B = 0 or $\sin\beta\ell = 0$.

Hence for a finite solution put B = 0.

$$\therefore y = \frac{w_0\pi^2}{\pi^2 - \beta^2\ell^2}\sin\frac{\pi x}{\ell}$$

or $$y = \frac{1}{1 - \left(\frac{\beta\ell}{\pi}\right)^2} w_0 \sin\frac{\pi x}{\ell} .$$

But $\left(\frac{\beta\ell}{\pi}\right)^2 = \frac{P\ell^2}{\pi^2 EI} = \frac{P}{P_c}$

where P_c is the Euler load,

$$\therefore y = \left[1/\left(1 - \frac{P}{P_c}\right)\right] w_0 \sin\frac{\pi x}{\ell} .$$

Hence the deflection curve for a column with initial curvature can be obtained by multiplying the deflection curve of an initially straight column by the "magnification factor" $\frac{1}{1-\frac{P}{P_c}}$.

Comparing the results of examples (a) and (b), the similarity in form of the resonance factor and magnification factor is evident. By extending the above simple analyses to the vibration of a beam under an arbitrary load distribution, and to the buckling of a column with an arbitrary initial curvature, it can be shown that identically similar factors occur. (References 1 and 2). It is this similarity that might lead one to suspect some connection between P_c and ω_o^2. The suspicion can be corroborated quite readily in the case of a beam which is pinned at each end. Without any external forces being applied to the system, the equation governing the free harmonic vibrations is

$$EI \frac{d^4w}{dx^4} - \rho w \omega^2 = 0.$$

The modes of vibration are given by

$$w = A_n \sin \frac{n\pi x}{\ell}$$

and the corresponding frequencies of vibration are

$$\omega_n = \frac{n^2\pi^2}{\ell^2}\sqrt{\frac{EI}{\rho}} .$$

Now consider an axial compression P acting along the center line of the beam. The corresponding equation for free vibrations becomes

$$EI \frac{d^4w}{dx^4} + P \frac{d^2w}{dx^2} - \rho w \omega^2 = 0.$$

The shape of the modes is the same as before, but the frequency is now

$$\omega_n = \frac{n^2\pi^2}{\ell^2} \sqrt{\frac{EI}{\rho}\left(1 - \frac{P}{P_n}\right)}$$

where $P_n = \frac{n^2\pi^2 EI}{\ell^2}$.

Hence the effect of the axial compression P is to decrease the natural frequency of vibration. In addition, the variation of the square of the frequency with P is linear; and finally, the frequency falls to zero when P approaches P_n which is the buckling load of the beam.

The question naturally arises as to the generality of this variation, and whether such a behavior can be expected in structures other than simply supported uniform beams. Physical intuition would lead one to believe that, if an axial compression does decrease the natural frequency, then the frequency of any structure would fall to zero when buckling is reached.

A review of the literature dealing with this problem reveals the sparseness of information which is available. By far the most extensive work is that by Massonnet (Reference 3), which was published in Belgium in 1940. Massonnet's paper is entirely theoretical, and he does derive some general relationships using

the energy approach. The greater portion of his paper is confined to the solution, by the differential equation method, of a large number of particular cases. He treats uniform beams, plates, rings and shells, and solves a great number of these with various boundary conditions.

An earlier treatise which was restricted to the vibrations and buckling of rectangular plates was published in Sweden in 1929 by Grauers (Reference 4). This is an exhaustive study of the vibrations of plates with various boundary conditions, in order to use these modes to find the stability criteria by Ritz's method. No attempt was made to draw any general conclusions between the vibration and stability problems.

A paper somewhat related to the present problem was published in this country by Weinstein and Chien (Reference 5), in which the vibrations of a clamped plate under tension were investigated. By using the variational energy approach, they showed that the square of the frequency of vibration increased with increased tension in an approximately linear manner.

Stephens (Reference 6) recognized the similarity between the stability and vibration problems, and proposed a method for determining the end fixity coefficient by a frequency measurement. His analysis, however, is based on a fallacious argument--this

is discussed more fully in Appendix C. He also proposed the frequency method for determining loads in axially stressed members, but here again his analysis errs. His paper does contain some useful experimental results on clamped bars.

The only other experimental work which seems to have been conducted is contained in a thesis by Chu (Reference 7). Guided by Massonnet's work, Chu tested a simply supported column and also a rectangular frame. His results for the column agreed very closely with theory. However, although he obtained a linear relationship between ω^2 and P for the rectangular frame, the extrapolated value of P_{cr} did not agree with the calculated lowest critical load corresponding to symmetrical buckling, but with a higher critical load which represented the unsymmetrical mode. Chu's work was not sufficiently complete to explain this phenomenon satisfactorily.

From the foregoing discussion, it is evident that the problem has by no means been thoroughly investigated. It is particularly desirable to know the restrictions under which the linear relationship holds, and, if the relationship is not linear under certain conditions, the deviation from linearity. In addition, some further experimental work appeared to be necessary. Firstly, Chu's work should be extended in order to understand the technique more fully, and secondly to attempt to check further theory.

The practical application of such information is two-fold. Firstly, the members of a structure are very often subjected to axial loads, and a determination of their natural frequency is of some significance in order to prevent resonance. Secondly, if such a law of variation of natural frequency with end thrust can be established, it would lead to useful practical applications in the form of non-destructive tests for the determination of the static buckling load.

It is the purpose of this work to explore, both theoretically and experimentally, the effect of axial loads on the frequency of vibration of elastic bodies.

PART II

GENERAL EQUATIONS

Before examining any specific class of elastic bodies, it is possible to study some general expressions which describe the vibrations of continuous systems such as beams and plates. The differential equation for the vibrations of such a system can be written in the general form

$$L[u] + c^2 u_{tt} = f(x_i;t) \tag{1}$$

where the subscript i takes on as many values as there are space variables. $L[u]$ is a linear differential expression which includes only the unknown deflection function u and its derivatives with respect to the space variables x_i. For example, for the uniform beam

$$L[u] = \frac{\partial^4 u}{\partial x^4} , \tag{2}$$

while for a plate of constant thickness

$$L[u] = \nabla^4 u. \tag{3}$$

In the above general equation, c^2 is a physical constant and $f(x_i;t)$ is proportional to the density of the external force.

In the problem under consideration the case of free vibrations is of primary interest. Mathematically this means that the

solution is given by a function u which satisfies the homogeneous differential equation

$$\mathcal{L}[u] + c^2 u_{tt} = 0 \tag{4}$$

together with the initial and boundary conditions of the problem.

In order to find the natural modes, the variables are separated by putting

$$u(x_i ; t) = w(x_i)\, g(t). \tag{5}$$

Substituting eq. (5) into eq. (4),

$$-\frac{\mathcal{L}[w]}{c^2 w} = \frac{g_{tt}}{g}.$$

Since the left side is a function of the space variables only, and the right side is a function only of time, it follows that each must be equal to a constant, say $-\omega^2$.

Hence the two total differential equations are obtained:

$$g_{tt} + \omega^2 g = 0 \tag{6}$$

$$\mathcal{L}[w] - \omega^2 c^2 w = 0. \tag{7}$$

The first equation yields solutions which are a harmonic function of time, while the solution of the latter (the eigenfunction equation) determines the admissable values of the constant ω^2 and hence the natural frequencies of the system.

Hence in general the natural frequencies will be given by the equation

$$\omega_n^2 = \frac{L[W_n]}{c^2 W_n} \quad . \tag{8}$$

A further and more complete treatment of the theory of eigenvalues is contained in Reference 8.

In the foregoing analysis it was assumed that no external forces were acting on the system. Now suppose that the vibrating system is subjected to an end load P. The only effect of this will be to modify the differential operator L. Denoting this modified operator by L* and the new deflection function by $v(x_i)$, the expressions (2) and (3) now become

$$L^*[V] = \frac{d^4V}{dx^4} + \frac{P}{EI}\frac{d^2V}{dx^2} \qquad \text{for beams} \tag{9}$$

$$\text{and } L^*[V] = \nabla^4 V + \frac{N_x}{D}\frac{\partial^2 V}{\partial x^2} + \frac{N_y}{D}\frac{\partial^2 V}{\partial y^2} \tag{10}$$

for plates subjected to end loads N_x and N_y per unit length. Eq. (8) now becomes

$$\omega_n^{*2} = \frac{L^*[V]}{c^2 V} \quad . \tag{11}$$

Hence from Eqs. (8) and (11) it can be concluded that

$$\left(\frac{\omega_n^*}{\omega_n}\right)^2 = \frac{W L^*[V]}{V L[W]} \quad . \tag{12}$$

As L* is a function of the end load, the right side of this equation will be a function of the end load. Hence Eq. (12) will give the general relationship between the square of the frequency and the end load. As w and v are both functions of x, Eq. (12) indicates that a necessary condition for $\left(\frac{\omega_n^*}{\omega_n}\right)^2$ to be proportional to the end load is that w(x) = v(x); i.e. the mode of free vibration must be unaltered by the application of an end load.

The value of the end load at which the natural frequency is reduced to zero can be deduced from Eq. (11). For ω_n^{*2} to be zero, L*[v] must vanish. Putting this condition in Eq. (9), the natural frequency of a beam will become zero when the end load assumes a value given by

$$\frac{d^4V}{dx^4} + \frac{P}{EI}\frac{d^2V}{dx^2} = 0. \tag{13}$$

But the values of P given by this equation correspond to the static buckling loads (See Appendix A). Hence the natural frequency is reduced to zero as the end load approaches the critical buckling load.

In precisely the same manner, if L* [v] vanishes in the case of plates, Eq. (10) yields

$$\nabla^4 V + \frac{N_x}{D}\frac{\partial^2 V}{\partial x^2} + \frac{N_y}{D}\frac{\partial^2 V}{\partial y^2} = 0. \tag{14}$$

Again the values of N_x and N_y as given by this equation correspond

to the static buckling loads of the plate (Reference 2).

Considering the other extreme case of the end thrust vanishing, Eqs. (9) and (10) simply reduce to Eqs. (2) and (3) respectively; viz. for normal free vibrations. From this, and the preceding results, the following conclusion can be deduced, bearing in mind the fact that the natural frequency of vibration is a function of the end load:

The most general expression for the shape of a beam or plate will be the mode of vibration with an end load; the free modes of vibration and the buckling modes are special limiting cases of this, viz. $P = 0$ and $\omega_n = 0$ respectively.

This reduces the apparently different physical problems of vibration and buckling to special cases of a single phenomenon. The mathematical similarity between the two problems has often been pointed out, but not the fact that they are limiting cases of the one problem.

PART III

THEORY OF STRAIGHT BEAMS

Having derived an expression relating the square of the frequency to the end load in very general terms, it is now advantageous to examine in greater detail the form that this equation assumes in the case of straight beams. At the same time it can be shown how the linear differential operators are obtained if the problem is begun from first principles.

The free vibrations of a beam are governed by the general beam equation

$$EI \frac{d^4 v}{dx^4} = p(x) \tag{15}$$

where p(x) is the loading per unit length. In the case of vibrations, this loading will correspond to the inertia loading $-\rho \frac{\partial^2 v}{\partial t^2}$. Hence by d'Alembert's principle, Eq. (15) can be written as

$$EI \frac{\partial^4 v}{\partial x^4} = -\rho \frac{\partial^2 v}{\partial t^2} .$$

Let $v(x,t) = w(x)\, g(t)$

$$\therefore EI \frac{\partial^4 w}{\partial x^4} g = -\rho w \frac{\partial^2 g}{\partial t^2}$$

$$\text{or } \frac{EI}{\rho w} \frac{\partial^4 w}{\partial x^4} = -\frac{1}{g} \frac{\partial^2 g}{\partial t^2} = \omega^2 .$$

Therefore this resolves into the two equations

$$g_{tt} + \omega^2 g = 0 \tag{16}$$

$$\& \quad \frac{d^4 W}{dx^4} - \frac{\rho}{EI} \omega^2 W = 0 . \tag{17}$$

Hence, in the notation of Eq. (7),

$$L[W] = \frac{d^4 W}{dx^4} \quad ; \quad c^2 = \frac{\rho}{EI} . \tag{18}$$

Now if an end thrust P is acting, the governing equation becomes

$$EI \frac{\partial^4 v}{\partial x^4} = -\rho \frac{\partial^2 v}{\partial t^2} + \frac{\partial^2 M_P}{\partial x^2}$$

where M_P = Bending Moment due to $P = -Pv$

$$\therefore EI \frac{\partial^4 v}{\partial x^4} + P \frac{\partial^2 v}{\partial x^2} = -\rho \frac{\partial^2 v}{\partial t^2} .$$

Putting $v(x,t) = V(x) g(t)$

the equation becomes

$$EIg \frac{\partial^4 V}{\partial x^4} + Pg \frac{\partial^2 V}{\partial x^2} = -\rho V \frac{\partial^2 g}{\partial t^2} .$$

Similarly, this can now be resolved into the two equations

$$g_{tt} + \omega^{*2} g = 0 \tag{19}$$

$$\& \quad \frac{d^4 V}{dx^4} + \frac{P}{EI} \frac{d^2 V}{dx^2} - \frac{\rho}{EI} \omega^{*2} V = 0 . \tag{20}$$

Hence in this case,

$$\mathcal{L}^*[v] = \frac{d^4v}{dx^4} + \frac{P}{EI}\frac{d^2v}{dx^2} \; ; \quad c^2 = \frac{\rho}{EI} \; . \tag{21}$$

Therefore, from Eq. (12),

$$\left(\frac{\omega_n^*}{\omega_n}\right)^2 = \frac{w\left(\frac{d^4v}{dx^4} + \beta^2 \frac{d^2v}{dx^2}\right)}{v\frac{d^4w}{dx^4}} \tag{22}$$

where $\beta^2 = \frac{P}{EI}$.

As indicated in the previous section, the general solutions of both Eqs. (17) and (20) can be obtained by considering Eq. (20) only, and then putting P = 0 to arrive at the solution of Eq. (17).

The characteristic equation of Eq. (20) is

$$\lambda^4 + \beta^2\lambda^2 - c^2\omega^{*2} = 0$$

$$\therefore \lambda^2 = -\frac{\beta^2}{2} \pm \sqrt{\left(\frac{\beta^2}{2}\right)^2 + c^2\omega^{*2}} \; .$$

As the radical is always positive, the two values of λ^2 are real; one is positive and one negative.

$$\therefore v = A\cosh\lambda_1 x + B\sinh\lambda_1 x + C\cos\lambda_2 x + D\sin\lambda_2 x \tag{23}$$

where $\lambda_1 = \sqrt{-\frac{\beta^2}{2} + \sqrt{\left(\frac{\beta^2}{2}\right)^2 + c^2\omega^{*2}}}$

and $\lambda_2 = \sqrt{-\frac{\beta^2}{2} - \sqrt{\left(\frac{\beta^2}{2}\right)^2 + c^2\omega^{*2}}}$.

Hence it follows that

$$w = Q\cosh\lambda_3 x + R\sinh\lambda_3 x + S\cos\lambda_3 x + T\sin\lambda_3 x \qquad (24)$$

where $\lambda_3 = \sqrt[4]{c^2\omega^2} = \sqrt[4]{\frac{\rho\omega^2}{EI}}$.

An examination of Eqs. (23) and (24) shows that the two modes can be equal if either the hyperbolic or the trigonometric functions vanish. In addition, for the linear relationship to hold, Eq. (22) indicates that $\left(\frac{d^4v}{dx^4} + \beta^2\frac{d^2v}{dx^2}\right)$ must be linearly related to $\frac{d^4w}{dx^4}$. These two requirements are possible if v and w are either hyperbolic functions or sine functions. No physical boundary conditions will yield purely hyperbolic solutions, hence the sine solutions are the only possible conditions for linearity. These correspond to simply supported ends.

Hence consider the case of a simply supported beam in which the boundary conditions are

(i) $v = 0$ at $x = 0, \ell$

(ii) $\frac{d^2v}{dx^2} = 0$ at $x = 0, \ell$.

(i) gives $A = C = 0$

(ii) gives $\left.\begin{aligned} \lambda_2^2 B\sinh\lambda_1\ell + \lambda_2^2 D\sin\lambda_2\ell = 0 \\ \lambda_1^2 B\sinh\lambda_1\ell - \lambda_2^2 D\sin\lambda_2\ell = 0 \end{aligned}\right\}$

$$\therefore (\lambda_1^2 + \lambda_2^2) B\sinh\lambda_1\ell = 0$$

$$\therefore B = 0 .$$

Hence $\sin \lambda_2 \ell = 0$

$$\therefore \lambda_2 \ell = n\pi \qquad (n = 1, 2, 3, \cdots)$$

$$\therefore \lambda_2 = \frac{n\pi}{\ell} \ .$$

Hence $v(x) = w(x) = D \sin \frac{n\pi x}{\ell}$

and Eq. (22) becomes

$$\left(\frac{\omega_n^*}{\omega_n}\right)^2 = 1 + \beta^2 \frac{\frac{d^2w}{dx^2}}{\frac{d^4w}{dx^4}}$$

$$= 1 + \beta^2 \frac{-\frac{n^2\pi^2}{\ell^2}}{\frac{n^4\pi^4}{\ell^4}} = 1 - \frac{\beta^2 \ell^2}{n^2\pi^2}$$

$$\therefore \left(\frac{\omega_n^*}{\omega_n}\right)^2 = 1 - \frac{P\ell^2}{n^2\pi^2 EI}$$

or $$\left(\frac{\omega_n^*}{\omega_n}\right)^2 = 1 - \frac{P}{P_n} \qquad (25)$$

where $P_n = \frac{n^2\pi^2 EI}{\ell^2}$ = buckling load corresponding to n^{th} mode of buckling.

This illustrates that the square of the frequency varies linearly with the end thrust. For P = 0, the frequency becomes the natural frequency for free vibration; at zero frequency, the end thrust is equal to the buckling load.

The experimental implications of this result are quite considerable. By measuring the natural frequency of free vibration for such a beam, first with no end load and then with an end load which may be well below the buckling load, these two points can

be extrapolated by a straight line to intersect the P abscissa for zero ω^2. Then this value of P will correspond to the buckling load. Hence a non-destructive test can be conducted to establish the experimental value of the buckling load.

Chu (Reference 7) conducted such a test on a straight bar of rectangular cross-section, simply supported at the ends. He measured the frequency of lateral vibration for a number of end loads, and the linearity of the frequency^2-load curve was verified to within very close limits. The extrapolated critical load was within 1/2 $^o/o$ of the calculated value. He did not measure the buckling load.

If $v(x) \neq w(x)$, Eq. (22) indicates that the linear relationship between ω^2 and P will no longer be valid. However, in the previous section it was established that even in this case the frequency becomes the natural frequency for free vibration when $P = 0$; and that the end thrust is equal to the buckling load at zero frequency. The question now arises as to the magnitude of the deviation from linearity for other end conditions. It will be shown in the following section how energy considerations can be utilized to give an estimation of this deviation in general. However, at this point, it would be instructive to examine the relationship for particular widely differing end conditions.

Two cases chosen are a beam fixed at each end, and a

cantilever. Introducing the relevant boundary conditions into Eq. (23), the frequency equations are obtained as a function of the end load. Hence the curves of $\left(\frac{\omega_n^*}{\omega_n}\right)^2$ against P/P_n can be plotted. Fig. 1 shows these curves for the fundamental mode.

It can be seen that the deviation from linearity is small in these two cases. For a beam with elastically restrained ends, one would expect the deviation to be even smaller, the curve lying between those for the simply supported and clamped beams. If this deviation can be shown to be sufficiently small for all practical cases, then the foregoing experimental method could be extended to cases in which the end fixity coefficients were unknown.

PART IV

ENERGY METHODS

As an alternative approach to the differential equation method, the nature of the problem strongly suggests an analysis by means of energy considerations. The results of the previous section indicate that for any boundary conditions, the mode of static buckling does not differ appreciably from the mode of free vibration. Hence it would be profitable to examine the problem in the light of Rayleigh's principle which requires only a moderately accurate representation of the amplitudes of vibration in the fundamental mode.

The amplitudes assumed in Rayleigh's method actually correspond to a slightly constrained mode, the frequency of which can easily be determined by energy calculations. The frequency thus obtained cannot be less than the true fundamental frequency, and so the method gives an upper bound. By using Rayleigh's principle, the approximation to the fundamental frequency will be much closer than the approximation of the assumed amplitudes to the true amplitudes.

The energy method can also be used in a very simple manner to determine the lower bound. This is particularly true where a system is simultaneously subjected to different types of external forces, each of which if acting separately would

result in an eigenvalue problem. Then, in general, an inequality can be derived which relates the combined external forces to each of them acting separately. (Reference 9).

This method is thus appropriately applicable to the problem of the vibrations of a beam subjected to end thrust. Let a beam of arbitrary mass distribution be subjected to an end thrust P and hence have a lateral vibration frequency ω_n^*. The amounts of work done by the end thrust P and the inertia forces can be represented by PW_1 and $\omega_n^{*2} W_2$ respectively, where W_1 and W_2 depend only on the deformations. If V represents the strain energy, the exact critical condition is given by

$$V = PW_1 + \omega_n^{*2} W_2 \ . \tag{26}$$

Let P_n be the static buckling load for this beam, and ω_n the natural frequency of free vibration with no end load. The critical relations for these two cases are

$$V' = P_n W_1' \tag{27}$$

$$\text{and} \quad V'' = \omega_n^2 W_2''$$

when the primed quantities are calculated from the deformations appropriate to each type of external force. Hence it can be concluded from Rayleigh's principle that

$$V \geq P_n W_1$$

and $$V \geq \omega_n^2 W_2$$

i.e. $$W_1 \leq \frac{V}{P_n} \quad \text{and} \quad W_2 \leq \frac{V}{\omega_n^2} \ .$$

Hence

$$V \leq P \frac{V}{P_n} + \omega_n^{*2} \frac{V}{\omega_n^2}$$

or $$1 \leq \frac{P}{P_n} + \frac{\omega_n^{*2}}{\omega_n^2} \ . \qquad (28)$$

Eq. (28) gives a lower limit to the frequency of the axially loaded beam. The equality sign will hold if the modes are identical in all three cases. This checks the previous result obtained for uniform beams which are simply supported.

Now Rayleigh's principle can be made to yield an upper limit to the fundamental frequency by the use of an assumed mode of vibration. A reasonable assumption for this purpose is to suppose that the mode of vibration with end thrust is identical to the mode of static buckling. Consider the energy expressions:

Strain energy due to bending $= \frac{1}{2}\int_0^\ell EI\left(\frac{d^2v}{dx^2}\right)^2 dx$

Work done by end thrust $= \frac{1}{2} P \int_0^\ell \left(\frac{dv}{dx}\right)^2 dx \ .$

Hence total potential energy $= \frac{1}{2}\int_0^\ell EI\left(\frac{d^2v}{dx^2}\right)^2 dx - \frac{1}{2} P \int_0^\ell \left(\frac{dv}{dx}\right)^2 dx \ . \qquad (29)$

On the assumption of synchronous motion,

$$\text{kinetic energy} = \tfrac{1}{2}\omega^{*2}\int_0^\ell \rho v^2 dx . \tag{30}$$

Equating Eqs. (29) and (30),

$$\tfrac{1}{2}\int_0^\ell EI\left(\frac{d^2v}{dx^2}\right)^2 dx - \tfrac{1}{2}P\int_0^\ell \left(\frac{dv}{dx}\right)^2 dx = \tfrac{1}{2}\omega^{*2}\int_0^\ell \rho v^2 dx$$

$$\therefore \int_0^\ell EI\left(\frac{d^2v}{dx^2}\right)^2 dx = P\int_0^\ell \left(\frac{dv}{dx}\right)^2 dx + \omega^{*2}\int_0^\ell \rho v^2 dx . \tag{31}$$

This relationship is exact if v is the actual deflection function of the vibrating strut, i.e. that which satisfies the differential equation. However, it results in a good approximation if the differential equation is entirely disregarded and v is any function of x which satisfies the boundary conditions and which is a moderately accurate representation of the vibrating mode.

In any case, if v is chosen to be a normed deflection function, then the exact expression (31) becomes for uniform beams

$$\frac{\rho\omega^{*2}}{EI} = \int_0^\ell \left(\frac{d^2v}{dx^2}\right)^2 dx - \frac{P}{EI}\int_0^\ell \left(\frac{dv}{dx}\right)^2 dx .$$

By using an approximate function for v(x), the relationship becomes $\frac{\rho\omega^{*2}}{EI} \leqq \int_0^\ell \left(\frac{d^2v}{dx^2}\right)^2 dx - \frac{P}{EI}\int_0^\ell \left(\frac{dv}{dx}\right)^2 dx$

$$\text{or} \quad 1 \geqslant \frac{c^2\omega^{*2}}{\int_0^\ell \left(\frac{d^2v}{dx^2}\right)^2 dx} + \beta^2 \frac{\int_0^\ell \left(\frac{dv}{dx}\right)^2 dx}{\int_0^\ell \left(\frac{d^2v}{dx^2}\right)^2 dx} . \tag{32}$$

Eq. (32) gives an upper limit to the frequency of the axially loaded beam. Again the equality sign will hold only if the modes are identical, in which case it checks with Eq. (28).

As an example of this upper limit in a particular case, consider a beam fixed at each end. The buckling mode is

$$v = A\left(1 - \cos\frac{2\pi x}{\ell}\right).$$

Determine A for normalization.

$$\int_0^\ell A^2\left(1-\cos\frac{2\pi x}{\ell}\right)^2 dx = 1$$

$$\therefore\ A = \sqrt{\frac{2}{3\ell}}$$

$$\therefore\ \frac{dv}{dx} = \sqrt{\frac{2}{3\ell}}\cdot\frac{2\pi}{\ell}\sin\frac{2\pi x}{\ell}$$

$$\&\ \frac{d^2v}{dx^2} = \sqrt{\frac{2}{3\ell}}\cdot\frac{4\pi^2}{\ell^2}\cos\frac{2\pi x}{\ell}.$$

Hence $$\int_0^\ell\left(\frac{dv}{dx}\right)^2 dx = \int_0^\ell \frac{8\pi^2}{3\ell^3}\sin^2\frac{2\pi x}{\ell}\,dx$$

$$= \frac{4\pi^2}{3\ell^2}$$

and $$\int_0^\ell\left(\frac{d^2v}{dx^2}\right)^2 dx = \int_0^\ell \frac{32\pi^4}{3\ell^5}\cos^2\frac{2\pi x}{\ell}\,dx$$

$$= \frac{16\pi^4}{3\ell^4}.$$

$\therefore$ Eq. (32) becomes

$$1 \geq \frac{c^2\omega^{*2}}{16\pi^4/3\ell^4} + \beta^2\,\frac{4\pi^2/3\ell^2}{16\pi^4/3\ell^4}$$

$$\therefore\ 1 \geqslant \frac{3\rho\omega^{*2}\ell^4}{16\pi^4 EI} + \frac{P\ell^2}{4\pi^2 EI}\ . \qquad (33)$$

But for a clamped bar,

$$P = \frac{4\pi^2 EI}{\ell^2}$$

and $$\omega_1^2 = (22.4)^2 \frac{EI}{\rho \ell^4} .$$

$\therefore$ Eq. (33) can be written as

$$1 \geq 0.966 \left(\frac{\omega_1^*}{\omega_1}\right)^2 + \frac{P}{P_1} . \qquad (34)$$

If Eqs. (28) and (34) are plotted, as in Figure 2, the true curve of $\left(\frac{\omega_1^*}{\omega_1}\right)^2$ against P/P_1 will lie somewhere between the two plots. At P = 0, it has been shown that $\omega_1^* = \omega_1$, hence an estimate of the probable curve may be drawn. This is shown on the figure. It is noticed that the deviation from linearity is small.

In any similar calculation, the form of Eq. (34) will be the same. The coefficient of P/P_1 will always be unity, because the assumed shape is the buckling mode. Hence for any boundary conditions the curve corresponding to Eq. (34) can be obtained simply by calculating the point A in Figure 2, i.e. the natural free vibration of a beam using the buckling mode in the Rayleigh approximation. From Rayleigh's principle it is known that this point will lie very close to unity, and so it can be concluded that the deviation of the true curve from $\frac{P}{P_1} + \left(\frac{\omega_1^*}{\omega_1}\right)^2 = 1$ is always very small.

PART V

EXPERIMENTAL TESTS ON BEAMS

The experimental verification of the variation of frequency with end load for a simply supported beam was carried out by Chu (Reference 7), and for a fixed ended column by Stephens (Reference 6). In both cases very satisfactory agreement with the theory was obtained. In order to test elastically restrained columns, Chu investigated the case of a rectangular frame subjected to end thrusts. Although he obtained a linear relationship between the load and the square of the frequency, the results were not conclusive. Theoretically the frame should buckle in the lowest energy state, which corresponds to a symmetrical mode. However, the buckling load corresponding to the extrapolated value of Chu's curve was approximately equal to the critical load for unsymmetrical buckling.

The frame in Chu's tests was excited by striking one of the vertical members with a rubber mallet, and the frequency was measured by recording the output of electric strain gauges on an oscillograph. Due to local yielding at the knife edges under application of load, the damping increased to such an extent that the test could only be conducted up to approximately half the buckling load. Chu remarked that although the measurements indicated that the structure was stable in the unsymmetrical mode of vibration, one could not however conclude that the structure would

buckle in that mode first. He stated that its dominance might be purely because of the method of excitation and the support conditions.

In view of the above tests, it was decided to carry out further tests on a similar rectangular frame. However, the frame supports would be improved, and a more refined technique of excitation would be developed. It was considered desirable to conduct the tests right up to the physical buckling load in order to correlate the vibration mode with the actual buckling mode.

The frame was made of cold rolled steel strip, brazed together at the four corners. At each corner, on the center line of the vertical members, hardened steel knife edge seats were soft-soldered to the horizontal bars in order to reduce damping as much as possible. Figure 3 shows the details of the frame. The load was applied through 1/4 x 1/4 tool bits resting in small V-blocks. The top knife edges were carried by a heavy I-beam which was loaded at the center so as to divide the load equally between the two legs of the frame.

Instead of measuring the free vibrations of the frame, it was decided to build an oscillator which would impose an exciting force on the frame. By varying the frequency of the oscillator so as to develop resonance, the natural frequency could be determined at each loading increment.

This was arranged by constructing a magnetic circuit with an alternating flux. The core of the magnet was made of one inch square annealed steel with a center pole piece, and one of the vertical members of the frame formed the return path. The arrangement is shown in Figure 4. The coil was made of approximately 2000 turns of 20 gauge wire wound on a cardboard bobbin. The air gap between the core and the frame could be varied to give maximum power output.

A 30-watt power amplifier was built as a power supply, the output from which was connected to an audio-oscillator in order to be able to vary the frequency. The oscillator was a Hewlett Packard model 200D, with a frequency range from 7 to 70,000 cycles per second. The oscillator was connected directly to the coil. A number of taps were arranged on the output transformer of the power amplifier and the taps used were tested empirically in order to give optimum power.

In order to measure the frequency of vibration of the frame and also to determine resonance, dynamic strain gauges were attached to the vertical members of the frame as shown in Figure 4. The strain gauges were SR-4 gauges, type C1, manufactured by the Baldwin Locomotive Works. Gauges were attached to both vertical members in order to determine whether the frame was vibrating in the symmetrical or unsymmetrical modes. The usual method

of measuring the strains by use of a Wheatstone bridge circuit was discarded in favor of a potentiometer circuit, as shown in the sketch.

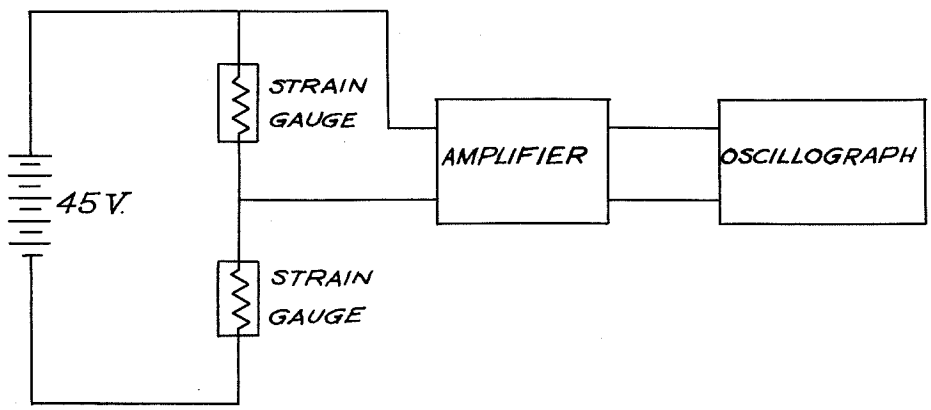

By having a strain gauge on each side of the bar, greatly increased sensitivity could be obtained and the necessity of having balancing resistances was obviated. A condenser in the amplifier blocks out the D.C. component of change of potential, and only the A.C. component due to the vibrating strain is transmitted to the oscillograph. The amplifiers and oscillograph were types BL202 and BL905 respectively, manufactured by the Brush Development Company. The oscillograph was a two-channel type with pen recorders, so that both vertical members could be recorded simultaneously.

The testing machine used was a hydraulic machine manufactured by the Tinius Olsen Testing Machine Company, and had a range up to 16,000 lb. in 20 lb. graduations. The complete set-up is shown in Figure 5.

The first test was conducted in order to determine whether Chu's results could be repeated. In his test the maximum load applied was below the critical load for symmetrical buckling. The first question to be settled was whether the frame, with an unsymmetrical stable vibration mode, would remain stable above the symmetrical buckling load.

Load was applied in 1000 lb. increments, and at each load the electro-magnet was energized. The frequency of the oscillator was varied until the occurrence of resonance, which was evidenced by maximum amplitude on the oscillograph. It was found that the frame vibrated in the unsymmetrical mode, corroborating Chu's results. The load was increased until it exceeded the theoretical symmetrical buckling load of 7330 lb., and the frame remained stable. Frequency measurements could be recorded above this load. In order to determine the mode of buckling, the load was increased continuously until instability resulted. It was found that the frame buckled in the unsymmetrical mode. The variation of frequency with load is shown as Curve 1 in Figure 6. Extrapolating the curve to zero frequency gives a buckling load of 11,150 lb., as compared to the theoretical unsymmetrical critical load of 11,360 lb. for this frame. The test also confirms that the deviation from linearity of the curve for such an elastically restrained strut is so small as to be negligible in comparison with experimental error.

Having established the fact that the mode of buckling is of the same form as the mode of vibration, a second test was conducted on a second frame of the same dimensions. Similar results occurred; the points are plotted as Curve 2 in Figure 6. The actual buckling load was measured as 10,250 lb., as compared with the extrapolated value of 11,450 lb. and the theoretical value of 11,360 lb. In this test an endeavor was made to obtain some points representing the symmetrical mode of vibration, but at most frequencies insufficient power was available. However, two points were obtained, and these are plotted as Curve 3 in Figure 6. The fact that this curve lies above that for unsymmetrical vibrations seems to imply that, for some reason, it is a higher energy state.

The third frame was constructed of similar dimensions, except that the knife edge seats were arranged eccentrically by moving them 0.2 inch towards the center line of the frame. This would ensure symmetrical buckling, and it was desired to determine the corresponding vibration modes. However, the vibrations were still unsymmetrical, and the points are plotted as Curve 4 in Figure 6. The measured buckling load was 5,500 lb.

It was significant that, in all three tests, the fundamental no-load frequency was approximately 100 cycles per second, corresponding to the symmetrical mode. (The unsymmetrical mode could also be excited at no load, but required more power.) As

soon as the first increment of load was applied, however, the stable mode became the unsymmetrical one.

In order to discover this apparent discrepancy with theory, it seemed logical to examine the experimental set-up in the light of the theoretical assumptions. The boundary conditions would first come under suspicion. All four knife edges were firmly supported in V-blocks which would prevent any lateral movement of the four corners. Although this appeared to be a minor point, the support system was modified. The two left-hand knife edge supports were 90° V-blocks as previously, but the right-hand supports were replaced by hardened steel knife edge seats. Also, the 1/4" x 1/4" knife edges were replaced by 1" x 1" tool steel knife edges. Hence lateral movement of the right-hand supports was now permitted. The modified system is shown in the following figure.

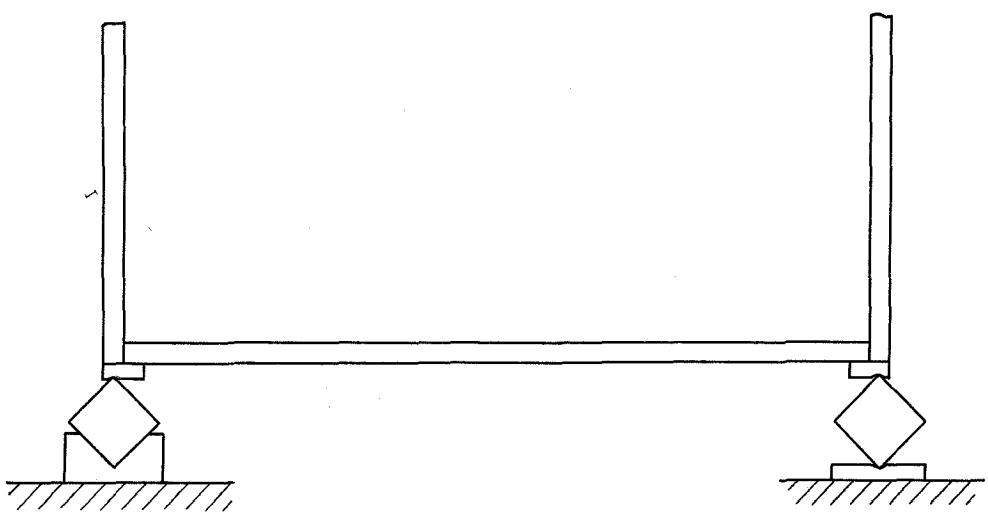

The frame tested with the modified boundary conditions was identical to those in the first two tests. Again load was applied in 1000 lb. increments. This time, however, the symmetrical mode became the stable configuration for all loads. The variation of frequency with load is shown as Curve 5 in Figure 6. Again linearity is verified to within experimental limits, the extrapolated value of 7330 lb. corresponding exactly to the theoretical buckling load. The frame actually failed at 6950 lb. in the symmetrical mode. In this test the unsymmetrical mode could also be excited with little difficulty, and by plotting these points the unsymmetrical buckling load could be estimated. This of course would not be of much practical significance as the frame is unstable above the symmetrical buckling load.

In view of the results of this test, the reason for the behavior of the frames tested previously now becomes apparent. The second-order effect of maintaining the horizontal distance between the knife edges is sufficient to cause the unsymmetrical mode to be the stable mode both for vibrations and buckling. The no-load frequency for the previous frames corresponded to the symmetrical mode because the support restraint was relieved under no load. It might be mentioned here that if the frame is completely free at the top to move laterally, the antisymmetric

buckling configuration is theoretically associated with the lower buckling load (Reference 16).

These tests thus showed up the very important result that the buckling load of a frame can be predicted by simply measuring the frequency of vibration under various loads. The correct mode of buckling will automatically be satisfied due to the fact that the vibrations will also occur in that mode. For example, Chu (Reference 7), although he obtained the predicted linear relationship in his test, was not sure why the extrapolated value would not correspond to the theoretical buckling load. He suggested that it might be due to his method of excitation. It is seen now that his extrapolated value would in fact correspond to the actual critical load for his boundary conditions had he continued loading up to buckling.

Two very important points must be realized in using this experimental method. The first is that the members of the frame must be long enough to fail by elastic instability, i.e. no short column effects. Secondly, the boundary conditions must be such that they will not vary with loading. This second conditions is not important in static buckling tests, because the equivalent end fixity at buckling can be computed. However, in the dynamic tests, it is important that the boundary conditions for each vibration test be identical to the boundary conditions which would prevail if buckling were to occur.

PART VI

THIN PLATES OF CONSTANT THICKNESS

In Part III it was shown how the particular equations for a straight beam were developed, and that these equations led to load-frequency^2 relationships which were either exactly or approximately linear. Proceeding in a similar manner, it is possible to derive the corresponding equations for a flat plate.

The free vibrations of a plate are governed by the general plate equation (Reference 2)

$$\nabla^4 U = \frac{\partial^4 U}{\partial x^4} + 2\frac{\partial^4 U}{\partial x^2 \partial y^2} + \frac{\partial^4 U}{\partial y^4} = \frac{q}{D} \tag{35}$$

where D is the flexural rigidity $= \frac{Eh^3}{12(1-\nu^2)}$, and q is the load per unit area. In order to extend this equation of equilibrium to that of motion, it is sufficient, by d'Alembert's principle, to replace q(x,y) by $-\mu \frac{\partial^2 U}{\partial t^2}$ where $\mu(x,y)$ is the mass per unit area. Then the equation for the vibrations of the plate becomes

$$\frac{\partial^4 U}{\partial x^4} + 2\frac{\partial^4 U}{\partial x^2 \partial y^2} + \frac{\partial^4 U}{\partial y^4} + \frac{\mu}{D}\frac{\partial^2 U}{\partial t^2} = 0. \tag{36}$$

Let $U(x,y;t) = W(x,y)\,g(t)$,

$$\therefore g(t)\nabla^4 W(x,y) + \frac{\mu}{D} W(x,y) g_{tt}(t) = 0,$$

$$\therefore \frac{D}{\mu}\frac{\nabla^4 W}{W} = -\frac{g_{tt}}{g} = \omega^2$$

Resolving this into two equations,

$$g_{tt} + \omega^2 g = 0 \tag{37}$$

and $$\nabla^4 w - \frac{\mu}{D}\omega^2 w = 0. \tag{38}$$

Hence, in the notation of Eq. (7),

$$L[w] = \nabla^4 w \; ; \; c^2 = \frac{\mu}{D} \; . \tag{39}$$

If the plate is subjected to compressive end thrusts N_x and N_y per unit length, and end shears N_{xy} per unit length, the dynamic equation becomes

$$\nabla^4 v = \frac{1}{D}\left[N_{xy}\frac{\partial^2 v}{\partial x \partial y} - N_x \frac{\partial^2 v}{\partial x^2} - N_y \frac{\partial^2 v}{\partial y^2} - \mu \frac{\partial^2 v}{\partial t^2}\right] . \tag{40}$$

Putting $v(x,y;t) = V(x,y)\, g(t)$

the equation becomes

$$g(t)\nabla^4 V(x,y) + \frac{1}{D} g(t)\left[N_x \frac{\partial^2 V}{\partial x^2} + N_y \frac{\partial^2 V}{\partial y^2} - N_{xy}\frac{\partial^2 V}{\partial x \partial y}\right] + \frac{\mu}{D} V(x,y)\frac{\partial^2 g}{\partial t^2} = 0$$

$$\therefore \frac{D}{\mu}\frac{\nabla^4 V}{V} + \frac{1}{\mu}\frac{1}{V}\left[N_x \frac{\partial^2 V}{\partial x^2} + N_y \frac{\partial^2 V}{\partial y^2} - N_{xy}\frac{\partial^2 V}{\partial x \partial y}\right] = -\frac{g_{tt}}{g} = \omega^{*2} .$$

This can be written as

$$g_{tt} + \omega^{*2} g = 0 \tag{41}$$

$$\epsilon \nabla^4 V + \frac{1}{D}\left[N_x \frac{\partial^2 V}{\partial x^2} + N_y \frac{\partial^2 V}{\partial y^2} - N_{xy} \frac{\partial^2 V}{\partial x \partial y} \right] - \frac{\mu}{D} \omega^{*2} V = 0 . \tag{42}$$

Hence

$$L^*[V] = \nabla^4 V + \frac{1}{D}\left[N_x \frac{\partial^2 V}{\partial x^2} + N_y \frac{\partial^2 V}{\partial y^2} - N_{xy} \frac{\partial^2 V}{\partial x \partial y} \right]$$

$$\epsilon C^2 = \frac{\mu}{D} . \tag{43}$$

The frequency relationship, from Eq. (12), then becomes

$$\left(\frac{\omega_n^*}{\omega_n}\right)^2 = \frac{W\left\{ \nabla^4 V + \frac{1}{D}\left[N_x \frac{\partial^2 V}{\partial x^2} + N_y \frac{\partial^2 V}{\partial y^2} - N_{xy} \frac{\partial^2 V}{\partial x \partial y} \right] \right\}}{V \nabla^4 W} . \tag{44}$$

If the plate is subjected to a thrust in the x-direction only, Eq. (44) reduces to

$$\left(\frac{\omega_n^*}{\omega_n}\right)^2 = \frac{W\left[\nabla^4 V + \frac{N_x}{D} \frac{\partial^2 V}{\partial x^2} \right]}{V \nabla^4 W} . \tag{45}$$

It is evident from Eq. (42) that, for a simply supported rectangular plate uniformly compressed in one direction, the solution can be written as

$$V(x,y) = A_{mn} \sin \frac{m\pi x}{a} \sin \frac{n\pi y}{b} .$$

As this mode would also satisfy Eq. (38), it can be concluded that Eq. (45) would yield a linear relationship between ω_n^2 and N_x .

However, there are less restrictive conditions under which this linear law is still exact. Consider a rectangular plate uniformly

compressed in the x-direction, simply supported along two opposite sides perpendicular to the direction of compression, and having various edge conditions along the other two sides. The equation of motion is then obtained from Eq. (42):

$$\nabla^4 V = \frac{1}{D}\left(-N_x \frac{\partial^2 V}{\partial x^2} + \mu\omega^{*2} V\right). \tag{46}$$

Assume a solution of the form

$$V = f(y) \sin \frac{m\pi x}{a} \tag{47}$$

which satisfies the boundary conditions along the simply supported edges x = 0, a. The f(y) will depend upon the other two boundary conditions. Substituting the value of v from Eq. (47) into Eq. (46), the differential equation for f(y) is obtained:

$$\frac{d^4 f}{dy^4} - \frac{2m^2\pi^2}{a^2}\frac{d^2 f}{dy^2} + \left(\frac{m^4\pi^4}{a^4} - \frac{N_x}{D}\frac{m^2\pi^2}{a^2} - \frac{\mu\omega^{*2}}{D}\right) f = 0 \ . \tag{48}$$

Noting that, owing to some constraints along the sides y = 0, b, one always has

$$\frac{N_x}{D}\frac{m^2\pi^2}{a^2} + \frac{\mu\omega^{*2}}{D} \geq \frac{m^4\pi^4}{a^4} \ ,$$

and using the notations

$$\alpha = \sqrt{\frac{m^2\pi^2}{a^2} + \sqrt{\frac{N_x}{D}\frac{m^2\pi^2}{a^2} + \frac{\mu\omega^{*2}}{D}}}$$

$$\beta = \sqrt{-\frac{m^2\pi^2}{a^2} + \sqrt{\frac{N_x}{D}\frac{m^2\pi^2}{a^2} + \frac{\mu\omega^{*2}}{D}}} \ , \tag{49}$$

the general solution of Eq. (48) can be represented in the following form:

$$f(y) = C_1 \cosh \alpha y + C_2 \sinh \alpha y + C_3 \cos \beta y + C_4 \sin \beta y . \tag{50}$$

If the homogeneous boundary conditions along the sides y = 0, b are substituted into this equation, the frequency equation is obtained. It is evident that this frequency equation will be a function of α and β only, yielding non-zero solutions α_i and β_i. Hence, irrespective of the value of the end thrust, the values of α_i and β_i are determined solely by the boundary conditions. Therefore, from Eqs. (49),

$$\pm \frac{m^2\pi^2}{a^2} + \sqrt{\frac{N_{x_i}^{cr}}{D} \frac{m^2\pi^2}{a^2}} = \pm \frac{m^2\pi^2}{a^2} + \sqrt{\frac{\mu \omega_i^2}{D}}$$

$$\therefore \omega_i^2 = \frac{N_{x_i}^{cr}}{\mu} \frac{m^2\pi^2}{a^2} . \tag{51}$$

Also, from Eqs. (49), one may write

$$\pm \frac{m^2\pi^2}{a^2} + \sqrt{\frac{N_x}{D} \frac{m^2\pi^2}{a^2} + \frac{\mu \omega_i^{*2}}{D}} = \pm \frac{m^2\pi^2}{a^2} + \sqrt{\frac{N_{x_i}^{cr}}{D} \frac{m^2\pi^2}{a^2}}$$

$$\therefore \omega_i^{*2} = \frac{m^2\pi^2 N_{x_i}^{cr}}{a^2 \mu} \left(1 - \frac{N_x}{N_{x_i}^{cr}}\right) .$$

Substituting from Eq. (51),

$$\left(\frac{\omega_i^*}{\omega_i}\right)^2 = 1 - \frac{N_x}{N_{x_i}^{cr}} . \tag{52}$$

Hence, provided the rectangular plate is simply supported along the two loaded edges, the linear relationship is true for any boundary conditions along the unloaded edges.

It was stated earlier that the condition for the linear relationship to be valid is that the buckling mode of an elastic body should be identical to the mode of free vibration. This is true for all plates of polygonal shape uniformly compressed in their median plane and simply supported along their edges. The normal vibration modes of such a plate are independent of the compression per unit length; they are identical to the normal modes of vibration of a membrane of the same shape and stretched uniformly, in addition to being identical to the buckling modes of the plate. The proof of this, which follows, is due to Shaefer and Havers (Reference 10).

For a simply supported plate, the boundary conditions are

$$V = 0$$

$$\text{and } \frac{\partial^2 V}{\partial n^2} + \nu \frac{\partial^2 V}{\partial t^2} = 0.$$

For a rectilinear contour $\frac{\partial^2 V}{\partial t^2} = 0$,

$$\therefore \frac{\partial^2 V}{\partial n^2} = 0 .$$

Hence the boundary conditions can be written as the so-called Navier boundary conditions

$$\nabla^2 V = 0$$

$$\text{and } V = 0 . \qquad (53)$$

For uniform compression,

$$N_x = N_y = N \; ; \quad N_{xy} = 0 .$$

$\therefore$ Eq. (42) becomes

$$\nabla^4 V + \frac{N}{D} \nabla^2 V - \frac{\mu}{D} \omega^{*2} V = 0 . \tag{54}$$

Writing $B_1 = \frac{N}{D}$ and $B_2 = \frac{\mu \omega^{*2}}{D}$, the equation becomes

$$\nabla^4 V + B_1 \nabla^2 V - B_2 V = 0$$

$$\therefore \nabla^2 (\nabla^2 V + C_1 V) + C_2 (\nabla^2 V + C_1 V) = 0$$

where $C_1 + C_2 = B_1$

$$\& \; C_1 C_2 = -B_2 \; .$$

Putting $$\phi = \nabla^2 V + C_1 V \tag{55}$$

the equation becomes

$$\nabla^2 \phi + C_2 \phi = 0 . \tag{56}$$

As B_2 is necessarily positive, C_1 and C_2 must be of opposite sign. Let C_1 be positive, C_2 negative.

The function ϕ which has to satisfy Eq. (56) is zero on the boundary. This follows from the definition of ϕ in Eq. (55), together with the Navier boundary conditions (53). From eigenfunction theory, Eq. (56) possesses non-zero solutions only for

certain positive values of C_2. As C_2 has been assumed negative, it necessarily follows that $\phi = 0$. The differential equation of the problem is then reduced to the second order equation (55):

$$\nabla^2 V + C_1 V = 0 \tag{57}$$

with v = 0 on the boundary.

But this is the governing equation for the vibrations of a membrane of the same shape as the plate. Eigenfunctions of the membrane are thus the same as for a vibrating plate ($C_1 = -C_2$), as well as for the stability problem ($C_2 = 0$). This proves the theorem.

Hence the following general result can be stated: For any thin plate of polygonal shape and uniform thickness which is simply supported along all the edges and subjected to a uniform thrust N per unit length, the frequency ω^* follows the relationship

$$\left(\frac{\omega_n^*}{\omega_n}\right)^2 = 1 - \frac{N}{N_n^{cr}} \quad .$$

It is interesting to note that although this relationship is exact for a polygonal plate with an arbitrarily large number of sides, it is not valid in the limit when the number of sides becomes infinite. The boundary would then be curved and the Navier boundary conditions would no longer be applicable.

Admittedly, however, the deviation from linearity in the case of a simply supported plate of arbitrary plan form would be expected to be very small. This can be seen very readily in the case of a circular plate; the normal modes of vibration and of buckling have been fully investigated in classical elasticity, and differ very little. However, it is curious that the exact linear law breaks down in the limit.

Plates with boundary conditions other than those already considered in this section can be treated very readily by the energy methods of Part IV. The lower limit of the frequency as given in Eq. (28) is still valid for plates. The upper limit can be computed by Rayleigh's principle, in which the energy expressions would be:

Strain energy due to bending =

$$\frac{1}{2} D \iint \left[\left(\frac{\partial^2 V}{\partial x^2} + \frac{\partial^2 V}{\partial y^2} \right)^2 - 2(1-\nu) \left\{ \frac{\partial^2 V}{\partial x^2} \frac{\partial^2 V}{\partial y^2} - \left(\frac{\partial^2 V}{\partial x \partial y} \right)^2 \right\} \right] dx\,dy$$

Work done by end thrusts =

$$\frac{1}{2} \iint \left[N_x \left(\frac{\partial V}{\partial x} \right)^2 + N_y \left(\frac{\partial V}{\partial y} \right)^2 - 2 N_{xy} \frac{\partial V}{\partial x} \frac{\partial V}{\partial y} \right] dx\,dy \,.$$

Hence the total potential energy, replacing Eq. (29), will be the difference between the above two expressions. The procedure would be identical to that in Section IV, viz. using a deflection function corresponding to the buckling mode. Hence similar

conclusions can be drawn: the actual load-frequency[2] curve will be bounded by lower and upper limits which, due to the nature of Rayleigh's method, will not differ greatly. Hence the deviation from linearity would be expected to be small. The actual limits can be computed for any particular boundary conditions merely by calculating the frequency of free vibration using the above energy method and using the deflection function of the buckling mode.

PART VII

EXPERIMENTAL TESTS ON PLATES

A survey of existing literature failed to yield any experimental data on the vibrations of rectangular plates. It appears that the only tests that have been carried out are on small circular plates for microphone diaphragms. Therefore it was decided to set up a testing program in which both unstiffened and stiffened flat plates could be loaded in compression while frequency measurements were made.

The plates to be used were made of 24 ST duralumin sheet, 12" x 12" x .040" thick. With simply supported edges, the buckling load for such a plate is approximately 200 lb., hence the dial of the testing machine would not be sensitive enough to record accurately the small load increments desired. A special ring gauge was used for this purpose, placed between the specimen and the platform of the testing machine. The ring gauge was constructed by using a 3" length of 10-3/4" O.D. seamless steel pipe 1/4" thick, and measuring its change of diameter under load by means of an Ames dial gauge calibrated in ten-thousandths of an inch. The ring gauge was accurately calibrated by loading it in increments with dead weight and noting the corresponding readings on the Ames gauge. The

load-deflection curve was linear, with each graduation of the Ames gauge being equivalent to approximately one pound. The ring gauge, mounted above the test specimen in the testing machine, is shown in Figure 7.

In order to vibrate the plate, a permanent magnet speaker with a rating of 20 watts was modified for the purpose. The loudspeaker was Type CMX-49155, manufactured by the Magnavox Company, and containing a heavy permanent magnet. Portions of the diaphragm were cut out in order to increase its flexibility, and an extension rod of aluminum was attached to the center of the diaphragm. This extension rod was then attached to the center of the plate by means of a rubber suction cup, with a small coil spring placed between them. This arrangement can also be seen in Figure 7. The voice coil of the speaker was energized from a power amplifier of 35 watt rating, with the Hewlett-Packard audio-oscillator put into the amplifier. Hence the diaphragm of the speaker could be made to vibrate at any frequency from about 10 cycles per second up.

The frequencies of the plate were measured by mounting pairs of SR-4 strain gauges on each side of the plate, and using a potentiometer circuit as described in Part V. The signals were automatically recorded by a recording oscilloscope manufactured by the William Miller Corporation (Model H).

The complete set-up is shown in Figure 8.

The first specimen to be tested was a simply supported flat plate. The four supports were V-grooves, and the edges of the plate were bevelled. As the maximum loading was to be of the order of 20 lb. per inch, hardened knife edges were not considered necessary. Increments of load were imposed on the plate, and at each loading the frequency of the oscillator was adjusted to make the plate resonate. The fundamental frequency could be detected quite readily.

However, the frequency remained approximately constant with load, increasing very slightly. For example, the fundamental frequency of the unloaded plate was 43 cycles per second, increasing steadily to 48 cycles per second at the theoretical buckling load of 200 lb. The test was repeated for a second and third plate, and in each case the frequency failed to decrease according to the theoretical analysis. In an effort to determine whether the boundary conditions were the cause of the trouble, steel knife edges were fitted along all four edges, and the test was repeated. This time the frequency did decrease slightly with load, but still bore no resemblance to the theoretical straight line. The points are plotted in Figure 9, Curve A.

Tests were then conducted on similar plates which, loaded along clamped edges, had the unloaded edges supported on knife

edges. Similar results were obtained, and these are shown in Figure 9, Curve B. The natural frequency for zero load was calculated by the method described in Appendix B. In the following tests, all four edges were clamped, with similar results.

In order to check the reliability of the oscillator, the two unloaded edges were allowed to deflect with no restraint, the loaded edges only being clamped. In this case the approximately linear theoretical curve was very closely followed, a result to be expected due to the fact that such a plate acts as a wide simple column. These points are also plotted in Figure 9, Curve C.

A series of tests were then conducted on a stiffened panel. The plate was of the same dimensions as the unstiffened plate, with the addition of a single channel stiffener rivetted longitudinally along the center of the plate. Tests were conducted with various edge conditions, but the results were very similar to those for the unstiffened plates.

As a result of the foregoing tests, it appears that thin plates under compression do not follow the linear load-frequency^2 relation in practice. A possible explanation might be that a thin plate is never perfectly flat, so that initial curvature in the plate may have some effect.

The effect of initial curvature may be investigated by the

linearized equations if the deflections are small in comparison with the thickness of the plate.

Let $v_o(x,y)$ = initial deflection function,

$v_1(x,y)$ = additional deflection after the application of N_x,

$v_2(x,y)$ = additional deflection due to vibrations.

Under static load, the differential equation becomes

$$\nabla^4 V_1 = \frac{1}{D}\left[-N_x \frac{\partial^2 (V_o + V_1)}{\partial x^2}\right] . \tag{58}$$

If the plate is vibrating, then the differential equation is

$$\nabla^4 (V_1 + V_2) = \frac{1}{D}\left[-N_x \frac{\partial^2 (V_o + V_1 + V_2)}{\partial x^2} - \mu \frac{\partial^2 V_2}{\partial t^2}\right] . \tag{59}$$

Subtracting Eq. (58) from Eq. (59),

$$\nabla^4 V_2 = \frac{1}{D}\left[-N_x \frac{\partial^2 V_2}{\partial x^2} - \mu \frac{\partial^2 V_2}{\partial t^2}\right] \tag{60}$$

which is identical to Eq. (40) for flat plates. This proves that for a thin plate with small initial curvature, the variation of frequency of lateral vibrations with edge thrust is identical to that of the corresponding flat plate. The two systems have, in particular, the same buckling load; and, moreover, the modes of vibration of the two systems (measured from the mean position) are identical.

The fact that the experimental data did not verify this result indicates that the deviation from flatness was not sufficiently small to justify the use of the linearized equations. The tests indicated

very clearly that the buckles grow with the beginning of loading, and gradually increase. This fact was also borne out in a paper by Hu, Lundquist and Batdorf (Reference 11), who showed theoretically that the Karman large-deflection equations should be used in studying the effect of small deviations from flatness on the buckling of plates in compression. The present tests also verified their conclusion that the Southwell method of predicting the theoretical critical stresses does not give satisfactory results, due to the fact that this method is based on the linear equations.

In a recent paper by Massonnet (Reference 12), a theoretical relationship between the frequency and end thrust was obtained for the case of circular plates with initial curvature. Using the Karman non-linear plate equations, Massonnet obtained an approximate solution for a clamped circular plate uniformly loaded around the circumference. The load-frequency relationship was computed for various initial deflections of the plate, and his results are plotted in Figure 10. The curves are plotted for various values of a parameter proportional to the initial deflection δ_o, viz. $\delta_o/2\sqrt{12(1-\nu^2)}h$. For example, the parameter equal to 1 corresponds to an initial deflection of 0.012 in. for 0.040 in. sheet. Massonnet's results confirm the experimental results as shown in Figure 9, and lend credence to the conclusion that

the initial curvature in the plate caused the considerable deviation from linearity.

It is therefore inferred that the justification for using the linear equations in such cases is not upheld in practice. The method of using frequency measurements in order to estimate the buckling load can not be expected to give satisfactory results in the case of plates in compression--at least in the case of aircraft panels, where the deviation from flatness may be of the same order as the thickness of the panel.

A possible way to eliminate the difficulty might be to test the plates in tension, measuring the frequency with each increment of load. In this case any initial curvature will be decreased with increasing load, and the linear equations may be valid. Extrapolation to zero frequency along the negative load axis would thus give the theoretical buckling load.

PART VIII

APPLICATION TO RIGID-JOINT FRAMES

In the previous sections it was pointed out that the approximately linear relationship between the load and the square of the frequency could only be expected to apply to elastic bodies whose boundary conditions did not vary with load. The rectangular frame which was tested (see Part V) complied with this condition as the horizontal members carried no load, and hence the buckling vertical members were restrained by the constant elastic restraints provided by the horizontal members. In the case of a rigid-joint truss, however, the axial force in each member increases with increasing load, and hence the effective rigidity at the end of any particular member does not remain constant. Consequently the deviation from the linear relationship cannot be expected to remain small in such a structure.

In order to ascertain the effect of the change of end restraint with load, it was decided to conduct tests on simple rigid-joint trusses. The truss configuration which was chosen is shown diagramatically in the following figure:

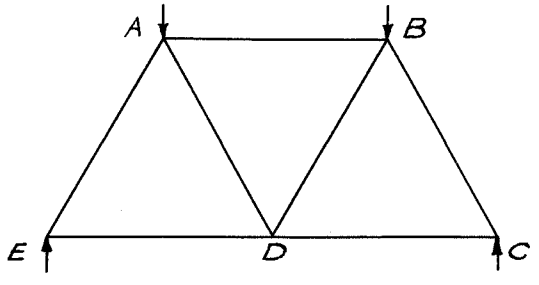

The members were all of the same length and rectangular in section. As the theory applies only to purely elastic instability, the length of the members was chosen with an ℓ/r ratio of at least 120 based on an effective length of $(3/4)\ell$. This resulted in the length being 12 in. for a thickness of 1/4 in. The width of the first frame tested was also 1/4 in. The material was mild steel, and all joints were brazed to make rigid connections.

Hardened steel knife edge seats were soldered to the horizontal bars at A, B, C and E, and 1/4 in. square tool steel bits were employed as knife edges. The knife edges at A and C were fixed, while those at B and E were allowed to pivot allowing lateral motion at those points. In the construction of the frame, considerable care was taken to ensure that the center lines of all members meeting at a joint did intersect at one point, and the knife edge seats on the frame were attached exactly above these points of intersection. The distance between knife edge seats on the loading platforms were adjustable so as to make certain that the load was being applied exactly vertically.

The frame was excited by attaching the vibrator described in Part VII to the center of, and normal to, the member AE in the plane of the truss. The frequency of vibration was measured by dynamic strain gauges attached to the members AB, BC and BD, and recording the output on the Miller oscillograph. The complete

test set-up is shown in Figure 11.

The frame was then loaded in 200 lb. increments, and the lowest resonant frequency recorded at each load. It was found that each of the instrumented members had a different resonant frequency for a particular load on the truss, but in addition there was one frequency at which all the members resonated. This resonant frequency for the complete truss was the one which decreased systematically with load, while the individual frequencies seemed to vary little. The load was increased until, at 1880 lb., the frame suddenly failed by torsional instability out of its plane. This unexpected failure prevented the test from being continued to the desired failure in the plane of the truss. The test results are plotted in Figure 12 as Curve 1.

A second frame was then constructed identical to the first, with the exception that the members were twice as wide, viz. 1/2 in. x 1/4 in. In addition, lateral restraint was provided by denying the top loading bar any possible angular rotation. These restraints can be seen in Figure 11. The frame was loaded in 400 lb. increments, and again the lowest resonant frequency for the complete frame was recorded at each load. The frame failed at 4945 lb., when the member AE began buckling in the plane of the truss. The test results are plotted in Figure 12 as Curve 2.

As would be expected, in analyzing the data it was found that at resonance all the members vibrated either in phase or 180° out of phase. From the diagram, it will be noticed that the frequency corresponding to 4400 lb. does not lie on the curve. This is due to the fact that at this load the exact resonance frequency was apparently not recorded, as the record showed that the vibrations for the members were definitely out of phase. As the square of the frequency is plotted, such small errors are considerably magnified.

The actual buckling load was lower than the extrapolated value of approximately 5600 lb., and this is apparently due to slight imperfections in the truss. It will be recalled that in the tests on rectangular frames, the actual buckling load was always lower than the extrapolated value. However, the latter value always agreed very closely with the theoretical buckling load. The theoretical buckling load for this truss was computed by a method developed by Winter (Reference 13) and extended by Bijlaard (Reference 14), and yielded a value of 4150 lb. That the carrying capacity of this truss would exceed this value was again to be expected in view of the fact that the two points A and C were prevented from moving, whereas the theory assumes only one restraint. The two restraints were necessary in order to prevent undue complication in the test set-up.

An examination of Figure 12 yields some interesting results. As predicted, the relationship is not linear. But more significant is the fact that the deviation from linearity is considerably larger in Curve 2. It might seem reasonable to deduce from these tests that the deviation from linearity increases as the section modulus of the members increases. This could be interpreted physically as follows. For a given moment of inertia, as the depth of the members is increased, the change in the end restraints due to axial loads in adjoining members is decreased.

In conclusion, some general remarks are in order regarding the applicability of the method as an experimental technique in practice. Provided that the end conditions do not vary with load, a straight line extrapolation will give good approximations to the buckling load of beams with arbitrary boundary conditions. On the other hand, the method does not seem to have any practical application in the case of flat plates because of the relatively large initial deflections encountered in practice. Tension tests may be successful. In connection with rigid-joint trusses, the method might be applicable under restricted conditions. Specialized research in this direction would be valuable in determining these limitations. For example, if some sort of symmetry could be established for the curvature of the load-frequency^2 curve, then the buckling load could be predicted from tests up to approximately half that load.

REFERENCES

1. Karman, Th. von & Biot, M.A.: Mathematical Methods in Engineering. McGraw-Hill Book Company. 1940.

2. Southwell, R. V.: Theory of Elasticity. Oxford University Press. 1941.

3. Massonnet, Ch.: Les Relations entre les Modes Normaux de Vibration et la Stabilite des Systems Elastiques. Bulletin des Cours et des Laboratoires d'Essais des Constructions du Genie Civil et d''Hydraulique Fluviale. Tome I, Nos. 1 & 2. 1940. Brussel.

4. Grauers, Hugo: Transversalschwingungen rechteckiger Platten mit besonderer Rücksickt der Knickung. Ingeniorsvetenskapsakademiens, Handlinger Nr 98, 1929. Stockholm.

5. Weinstein, A. and Chien, W. Z.: On the Vibrations of a Clamped Plate under Tension. Quarterly of Applied Mathematics, Vol. 1, No. 1, 1943.

6. Stephens, B. C.: Natural Vibration Frequencies of Structural Members as an Indication of End Fixity and Magnitude of Stress. Journal of the Aeronautical Sciences, Vol. 4, No. 2, 1936.

7. Chu, T. H.: Determination of Buckling Loads by Frequency Measurements. Thesis at the California Institute of Technology, 1949.

8. Courant, R.: Advanced Methods in Applied Mathematics. New York University, 1941.

9. Temple, G. and Bickley, W. G.: Rayleigh's Principle. Oxford University Press. 1933.

10. Schaefer, H. and Havers, A.: Die Eigenschwingungen der in ihrer Ebene allseitig gleichmässig belasteten gleichseitigen Dreiecksplatte. Ingenieur-Archiv, Vol. 7, No. 1. 1936.

11. Hu, P. C., Lundquist, E. E. and Batdorf, S. B.: Effect of Small Deviations from Flatness on Effective Width and Buckling of Plates in Compression. N.A.C.A. Technical Note No. 1124, 1946.

12. Massonnet, Ch.: Le Voilement des Plaques Planes Sollicitees dans leur Plan. Final Report of the Third Congress of the International Association for Bridge and Structural Engineering. Liege, September 1948.

13. Winter, G., Hsu, P. T., Koo, B. and Loh, M. H.: Buckling of Trusses and Rigid Frames. Bulletin No. 36, Eng. Expt. Station, Cornell University, April 1948.

14. Bijlaard, P. P.: Investigation on Buckling of Rigid Joint Structures. First Progress Report, Department of Structural Engineering, Cornell University, November 1949. (Unpublished).

15. Timoshenko, S.: Theory of Elastic Stability. McGraw-Hill Book Company. 1936.

16. Hertwig, A., and Pohl, K.: Die Stabilität des Bruckenendrahmens. Stahlbau, Vol. 9, 1936, p. 129.

APPENDIX A

ELASTIC STABILITY OF STRUTS

Invariably the texts in Elasticity and Strength of Materials derive the stability criteria for struts by first setting up the beam bending moment equation

$$EI \frac{d^2V}{dx^2} = -M(x) \tag{A.1}$$

Depending upon the end fixity, the bending moment M is determined as a function of x. This equation is then solved as an eigenvalue problem for non-zero solutions, the boundary conditions providing the eigenvalue equation. In general, however, this procedure is too limited both physically and mathematically, and in some cases the correct approach yields additional results which normally would not become evident by using the classical method.

The lack of generality in Eq. (A.1) can be appreciated when it is realized that for any beam problem four boundary conditions are always available--two at each end. For example, the boundary conditions corresponding to the usual cases encountered in the tests are:

(a) pinned end: $V = 0 \; ; \; \frac{d^2V}{dx^2} = 0$ (A.2)

(b) fixed end: $V = 0 \; ; \; \frac{dV}{dx} = 0$ (A.3)

(c) free end: $\frac{d^2V}{dx^2} = 0 \; ; \; EI \frac{d^3V}{dx^3} + P\frac{dV}{dx} = 0.$ (A.4)

Being a second order differential equation, Eq. (A.1) is too limited to provide a general solution. Instead, the fundamental fourth order beam equation

$$\frac{d^2}{dx^2}\left(EI\,\frac{d^2V}{dx^2}\right) = p(x) \tag{A.5}$$

should be used. This makes the problem mathematically consistent, and also allows a general equation to be set up which is independent of the boundary conditions. This is important because it allows an equation to be formulated which is also independent of the mode of buckling. The only assumption regarding the mode is that equilibrium is possible for some shape other than the original straight form, provided the displacements are small.

In order to use Eq. (A.5), the axial force P must be replaced by an equivalent transverse load **p**(x). The axial force induces a bending moment Pv in the deflected column, and the load corresponding to this bending moment distribution M(x) is equal to

$$p(x) = -\frac{d^2M}{dx^2} .$$

Hence the equivalent lateral load which would produce a moment Pv is equal to

$$p(x) = -P\,\frac{d^2V}{dx^2} .$$

Therefore Eq. (A.5) becomes

$$\frac{d^2}{dx^2}\left(EI\,\frac{d^2V}{dx^2}\right) = -P\,\frac{d^2V}{dx^2} . \tag{A.6}$$

This equation, together with the relevant boundary conditions (A.2), (A.3) or (A.4), should be employed for the general solution of the column problem.

For a beam of constant section, Eq. (A.6) reduces to

$$\frac{d^4V}{dx^4} + \beta^2 \frac{d^2V}{dx^2} = 0 , \tag{A.7}$$

so that Eq. (A.7) is the fundamental equation for a uniform beam. This agrees with Eq. (20) in Part III if $\omega = 0$ in that equation.

A good example of the principles involved is provided by the case of a column fixed at both ends. Without considering any specific mode of buckling, the problem can be stated mathematically as the differential equation (A.7) together with the boundary conditions (A.3), i.e.

$$(V)_{x=0} = (V)_{x=\ell} = 0 ; \left(\frac{dV}{dx}\right)_{x=0} = \left(\frac{dV}{dx}\right)_{x=\ell} = 0 . \tag{A.8}$$

From Eq. (A.7),

$$\frac{d^2V}{dx^2} = A \cos \beta x + B \sin \beta x$$

$$\therefore V = -\frac{A}{\beta^2} \cos \beta x - \frac{B}{\beta^2} \sin \beta x + Cx + D . \tag{A.9}$$

Putting in the boundary conditions at x = 0,

$$0 = -\frac{A}{\beta^2} + D$$

$$0 = -\frac{B}{\beta} + C$$

$$\therefore V = \frac{A}{\beta^2}(1 - \cos \beta x) + \frac{B}{\beta^2}(\beta x - \sin \beta x) . \tag{A.10}$$

Putting in the boundary conditions at $x = \ell$,

$$0 = \frac{A}{\beta^2}(1-\cos\beta\ell) + \frac{B}{\beta^2}(\beta\ell - \sin\beta\ell) \tag{A.11}$$

$$0 = \frac{A}{\beta}\sin\beta\ell + \frac{B}{\beta}(1-\cos\beta\ell) . \tag{A.12}$$

For a solution, the determinant must be equal to zero.

$$\therefore (1-\cos\beta\ell)^2 - (\beta\ell - \sin\beta\ell)\sin\beta\ell = 0$$

$$\text{i.e.} \quad 2 - 2\cos\beta\ell - \beta\ell\sin\beta\ell = 0 . \tag{A.13}$$

The solution of this transcendental equation will give the values of β leading to the critical loads. Fig. 13 shows a plot of this equation, the zeros corresponding to the eigenvalues. Note that there is a sequence of solutions alternating with the classical solution of $\beta\ell = 2\pi n$.

The two sequences can be separated by rewriting Eq. (A.13) as

$$\sin\frac{\beta\ell}{2}\left(2\sin\frac{\beta\ell}{2} - \beta\ell\cos\frac{\beta\ell}{2}\right) = 0 .$$

$$\therefore \quad \text{either} \quad \sin\frac{\beta\ell}{2} = 0 \tag{A.14}$$

$$\text{or} \quad \tan\frac{\beta\ell}{2} = \frac{\beta\ell}{2} . \tag{A.15}$$

Eq. (A.14) yields the usual values of the critical load, viz.

$$P_{cr} = \frac{4\pi^2 n^2 EI}{\ell^2} \qquad (n = 1, 2, 3, \cdots) \tag{A.16}$$

Eq. (A.15) yields an additional sequence, the first three values of which are

$$\frac{\beta\ell}{2} = 4.494,\ 7.725,\ 10.904,\text{---} \tag{A.17}$$

$$\therefore P_{cr} = \frac{8.18\pi^2EI}{\ell^2},\ \frac{24.19\pi^2EI}{\ell^2},\ \frac{48.19\pi^2EI}{\ell^2},\ \cdots \tag{A.18}$$

The shape of the modes can be obtained directly by the usual methods. First consider the eigenfunctions obtained from Eq. (A.14). This equation leads to the eigenvalues

$$\frac{\beta\ell}{2} = n\pi$$

$$\therefore \beta_n = \frac{2n\pi}{\ell}.$$

Substituting these values of β in Eq. (A.11)

$$0 = \frac{A}{\beta_n^2}(1-\cos 2n\pi) + \frac{B}{\beta_n^2}(2n\pi - \sin 2n\pi)$$

$$= \frac{B}{\beta_n^2}(2n\pi)$$

$$\therefore B = 0.$$

$\therefore$ Eq. (A.10) becomes

$$V = \frac{A}{\beta^2}\left(1-\cos\frac{2n\pi x}{\ell}\right). \tag{A.19}$$

These modes are shown in Fig. 14, in which P_1 represents the Euler critical load π^2EI/ℓ^2. They are the modes corresponding to the classical critical loads. Note that as the bracket in Eq. (A.19) is always positive, the deflections must necessarily lie on one side of the undeflected shape.

Next consider the eigenfunctions obtained from Eq. (A.15). Let the sequence of numerical values for $\beta\ell/2$ be ϕ_n [Ref. Eq. (A.17)].

$$\therefore \beta_n = \frac{2\phi_n}{\ell} .$$

Substitute these values of β in Eq. (A.12).

$$0 = \frac{A}{\beta_n} \sin 2\phi_n + \frac{B}{\beta_n} (1 - \cos 2\phi_n)$$

$$\therefore \frac{A}{B} = -\tan \phi_n .$$

$\therefore$ = Eq. (A.10) becomes

$$V = C \left[\frac{2\phi_n x}{\ell} - \sin \frac{2\phi_n x}{\ell} - \tan \phi_n \left(1 - \cos \frac{2\phi_n x}{\ell}\right) \right] . \qquad (A.20)$$

These modes are shown in Fig. 15, in which again P_1 represents the Euler critical load. They are similar to the modes of a strut of which both ends are constrained to remain on a fixed line, one end being "fixed" and the other "pinned".

An important practical point immediately becomes apparent. Suppose such a clamped strut is to be used to carry a load greater than the lowest buckling load, and this is to be accomplished by restraining the center from lateral displacement. According to the classical formula, the strut will then carry a load of $16\pi^2 EI/\ell^2$ [n = 2 in Eq. (A.16)]. Actually, however, it will carry only $8.18\ \pi^2\ EI/\ell^2$ and buckle into the shape shown in

Fig. 15(a). This can be shown to represent a lower energy state than the mode of Fig. 14(b). Similarly, for all modes higher than the fundamental, the beam may buckle in the series given by Fig. 15 rather than Fig. 14 if only the stationary points are restrained from lateral displacement.

From a mathematical point of view, the reason has already been stated to explain why the classical approach fails to yield the complete solution. A fourth order differential equation must always be used in order to satisfy the four possible boundary conditions of a beam. From a physical point of view, the limitation was imposed on the original diagram from which the forces and moments were obtained. Fig. 16(a) shows this complete diagram. But consider a mode of the second sequence as shown in Fig. 16(b). Here the end moments are in the same direction, and shear reactions are necessary for equilibrium. If these reactions are included in the second order moment equation, this second type of mode will become apparent--but not the first. Only the fourth order equation will yield all possible modes.

APPENDIX B

NATURAL FREQUENCY OF RECTANGULAR PLATES WITH TWO OPPOSITE EDGES SIMPLY SUPPORTED

From a review of the literature it appears that very little work has been done on the vibrations of plates with mixed boundary conditions. Grauers (Reference 4) did consider some of these cases, but his method of presentation appears to be too cumbersome to be of practical use.

In view of the fact that the frequency and buckling problems for a plate are identical eigenvalue problems, it would seem very profitable to utilize for the vibration problem the large amount of data that the N.A.C.A. has computed for the buckling of plates. In particular, if two opposite edges are simply supported the analogy is extremely simple, no matter what the other two boundary conditions may be. In this Appendix the natural frequency will be determined as a function of the plate buckling factor k.

Let the rectangular plate be simply supported along the two edges x = 0 and x = a, and have various edge conditions along the other two edges y = 0 and y = b. From Eq. (48), the differential equation for f(y) for buckling is

$$\frac{d^4f}{dy^4} - \frac{2m^2\pi^2}{a^2}\frac{d^2f}{dy^2} + \left(\frac{m^4\pi^4}{a^4} - \frac{N_x}{D}\frac{m^2\pi^2}{a^2}\right)f = 0 \qquad \text{(B.1)}$$

while that for free vibrations becomes

$$\frac{d^4f}{dy^4} - \frac{2m^2\pi^2}{a^2}\frac{d^2f}{dy^2} + \left(\frac{m^4\pi^4}{a^4} - \frac{\mu\omega^2}{D}\right)f = 0 . \qquad (B.2)$$

Equation (50) will represent the general solution for both Eqs. (B.1) and (B.2) with the corresponding values for α and β . For buckling,

$$\alpha = \sqrt{\frac{m^2\pi^2}{a^2} + \sqrt{\frac{N_x}{D}\frac{m^2\pi^2}{a^2}}} \; ; \; \beta = \sqrt{-\frac{m^2\pi^2}{a^2} + \sqrt{\frac{N_x}{D}\frac{m^2\pi^2}{a^2}}} \qquad (B.3)$$

and for free vibrations,

$$\alpha = \sqrt{\frac{m^2\pi^2}{a^2} + \sqrt{\frac{\mu\omega^2}{D}}} \; ; \; \beta = \sqrt{-\frac{m^2\pi^2}{a^2} + \sqrt{\frac{\mu\omega^2}{D}}} . \qquad (B.4)$$

Considering the two edges y = 0 and y = b to have the same boundary conditions in the vibration case as in the buckling problem, the constants of integration in Eq. (50) will be identical in terms of α and β for the two problems. Hence, for equivalence, let

$$\frac{\mu\omega^2}{D} = \frac{N_x}{D}\frac{m^2\pi^2}{a^2} . \qquad (B.5)$$

The coefficient k for critical buckling (Reference 15) is defined as

$$N_x = k\frac{\pi^2 D}{b^2} . \qquad (B.6)$$

Substituting Eq. (B.6) into Eq. (B.5) yields

$$\omega^2 = \frac{m^2\pi^4 D}{\mu}\frac{k}{(ab)^2} . \qquad (B.7)$$

Hence for any boundary conditions along the edges y = 0 and y = b, the value of k can be obtained from Reference 15 or the various N.A.C.A. reports, and the natural frequency computed from Eq. (B.7).

In one respect the vibration problem differs from the buckling phenomenon, viz. that for the former the fundamental mode always corresponds to m = 1. Hence for the fundamental frequency Eq. (B.7) becomes

$$\omega^2 = \frac{\pi^4 D}{\mu} \frac{k}{(ab)^2} \tag{B.8}$$

where k is the buckling constant for m = 1. This may not necessarily correspond to the lowest value of k for a given a/b ratio, whereas in the case of buckling k and m are always chosen to give the lowest value of k.

APPENDIX C

END RESTRAINT AND NATURAL FREQUENCY

In Reference 6, Stephens proposed that the end restraint of a beam could be found by measuring the natural vibration frequency of the beam. The coefficient expressing this restraint is defined as the constant c in the basic Euler buckling equation

$$P_{cr} = \frac{c\pi^2 EI}{\ell^2} \quad . \tag{C.1}$$

To correlate the degree of end fixity with the natural frequency, Stephens used the value of c for the following four different types of end restraint:

(a) one end fixed, one end free ($c = 1/4$),

(b) both ends pinned ($c = 1$),

(c) one end fixed, one end pinned ($c = 2.047$),

(d) both ends fixed ($c = 4$).

The frequency equations for these four types of restraint were then calculated, and the first eigenvalue determined for each case. The square of the eigenvalue was called the "frequency constant", denoted by K. The values for K are 3.516, 9.870, 15.421 and 22.373 respectively for the above four cases. By plotting K against c, Stephens obtained a single curve. Thus to determine the degree of end restraint he stated that it was only necessary to determine the natural vibration frequency by test, after which K could be determined from the equation

$$f = \frac{K}{2\pi\ell^2}\sqrt{\frac{EI}{\rho}} \ .$$

The corresponding value of c, which is the measure of the end fixity, could then be found from the curve of K against c.

However, his proposed relationship between K and c is not unique, as there may be more than one value of K corresponding to each value of c. This might be suspected from the physics of the problem. It is quite feasible for two identical bars with differently restrained ends to have the same resultant fixity coefficient c. However, different modes of vibration, and hence different frequencies, would be anticipated.

A simple example will illustrate this. Consider a strut elastically restrained at each end, and suppose the restraint is such as to give an end fixity coefficient equal to 2.047 (the same as for one end fixed, one end pinned). The value of K for such a beam may be calculated. Suppose the spring constant at each end is the same, and denote it by α. Taking the origin of coordinates at the center of a beam of length 2L, the boundary conditions are:

(a) $\quad V = 0 \quad at \quad X = \pm L$ (C.2)

(b) $\quad EI\,V'' = \alpha V' \quad at \quad X = \pm L \ .$

The general solution of the buckling problem, as given by Eq. (A.9), is

$$V = A\cos\beta x + B\sin\beta x + Cx + D \qquad \text{(C.3)}$$

where $\beta^2 = \frac{P}{EI}$.

As $P = \frac{c\pi^2 EI}{4L^2}$,

$$\therefore \beta = \frac{\pi\sqrt{c}}{2L} . \qquad \text{(C.4)}$$

By symmetry, $B = C = 0$

$$\therefore V = A\cos\beta x + D .$$

Putting in the boundary conditions (C.2),

$$D = -A\cos\beta L$$

and

$$EI\alpha^{-1}(-A\beta^2\cos\beta L) = -A\beta\sin\beta L$$

$$\therefore \frac{EI}{\alpha}\beta = \tan\beta L .$$

Substituting the value for β from Eq. (C.4),

$$\alpha = \frac{\pi EI\sqrt{c}}{2L}\cot\frac{\pi\sqrt{c}}{2} . \qquad \text{(C.5)}$$

The general solution for free vibrations, from Eq. (24), is

$$V = A\cos\lambda x + B\sin\lambda x + C\cosh\lambda x + D\sinh\lambda x \qquad (C.6)$$

where $\lambda^2 = \omega\sqrt{\frac{\rho}{EI}}$.

By symmetry, $B = D = 0$.

$$\therefore V = A\cos\lambda x + C\cosh\lambda x .$$

Putting in the boundary conditions (C.2),

$$A = -C\,\frac{\cosh\lambda L}{\cos\lambda L}$$

$$\& \quad \frac{EI}{\alpha}(-A\lambda^2\cos\lambda L + C\lambda^2\cosh\lambda L) = -A\lambda\sin\lambda L + C\lambda\sinh\lambda L$$

$$\therefore \frac{EI\lambda}{\alpha}(2\cosh\lambda L) = \tan\lambda L\cosh\lambda L + \sinh\lambda L$$

$$\therefore \alpha = \frac{2EI\lambda}{\tan\lambda L + \tanh\lambda L} . \qquad (C.7)$$

As the value of α is to be the same for buckling and vibrations, Eqs. (C.5) and (C.7) may be equated

$$\therefore \frac{2\lambda L}{\tan\lambda L + \tanh\lambda L} = \frac{\pi\sqrt{c}}{2}\cot\frac{\pi\sqrt{c}}{2} . \qquad (C.8)$$

Taking c = 2.047 as for the fixed-pinned strut, Eq. (C.8) becomes

$$\frac{2\lambda L}{\tan \lambda L + \tanh \lambda L} = -1.8052$$

$$\therefore 2\lambda L = 3.776$$

$$\therefore K = (2\lambda L)^2 = 14.258.$$

Hence for a symmetric strut with elastically restrained ends, an end fixity coefficient of 2.047 corresponds to a frequency constant of 14.258; whereas for a fixed-pinned strut with the same end fixity coefficient, the frequency constant is 15.421. It may be concluded that Stephen's single curve relating c to K is not justifiable.

In the same paper, Stephens derives the relation between end thrust and vibration frequency as

$$P = mP_{cr}\left[1 - \left(\frac{f}{f_o}\right)^2\right]$$

where m is a constant depending on the end restraint. He lists m for various end conditions. This again is erroneous, as m is actually a function of P if the ends are not pinned. The constant m was determined by the energy method, which would naturally give the upper curve of Fig. 2. According to the above formula, $P \neq P_{cr}$ when $f = 0$. However, it was proved in Part II that as P is increased, f decreases until it finally vanishes at $P = P_{cr}$.

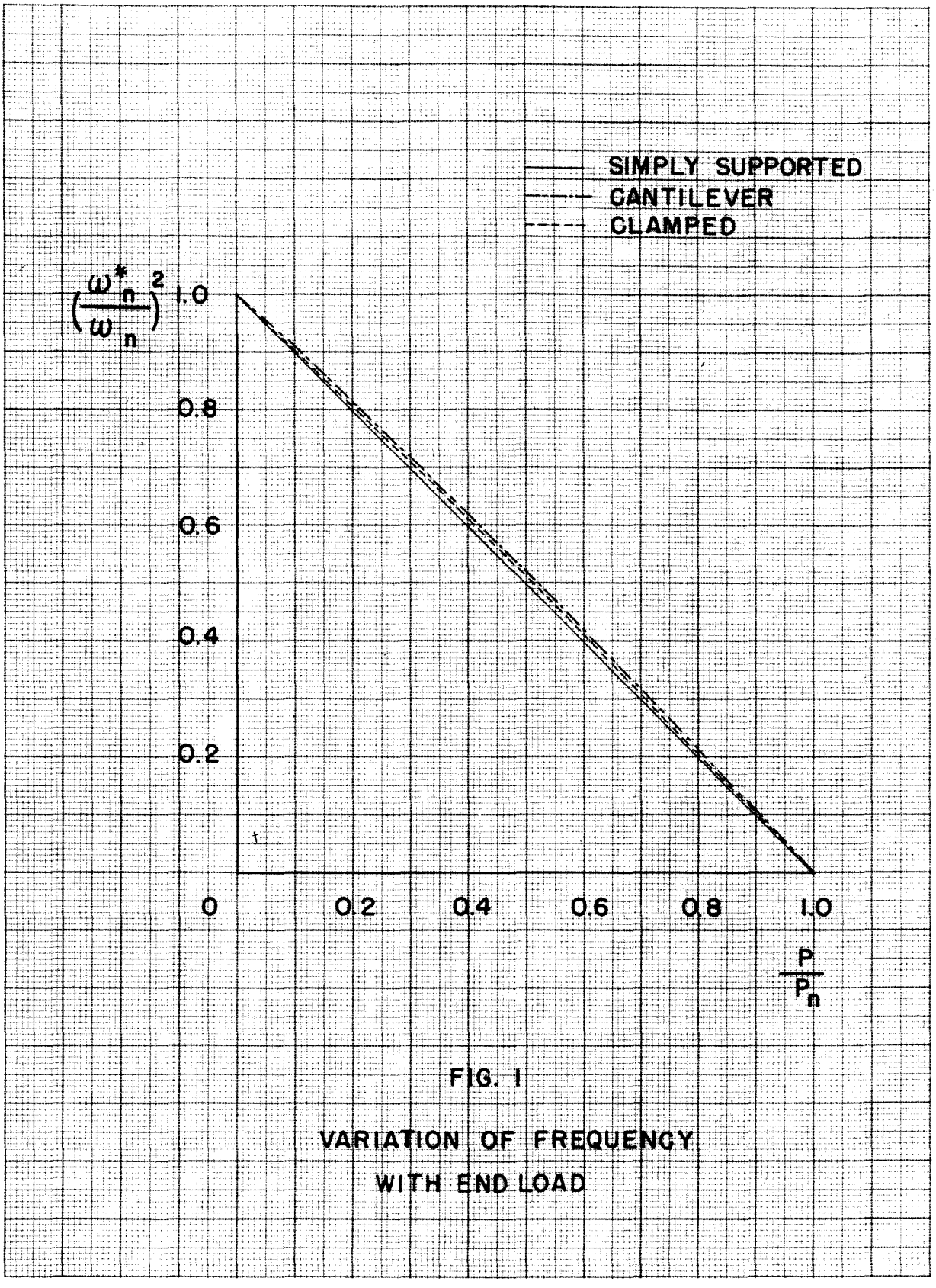

FIG. 1

VARIATION OF FREQUENCY WITH END LOAD

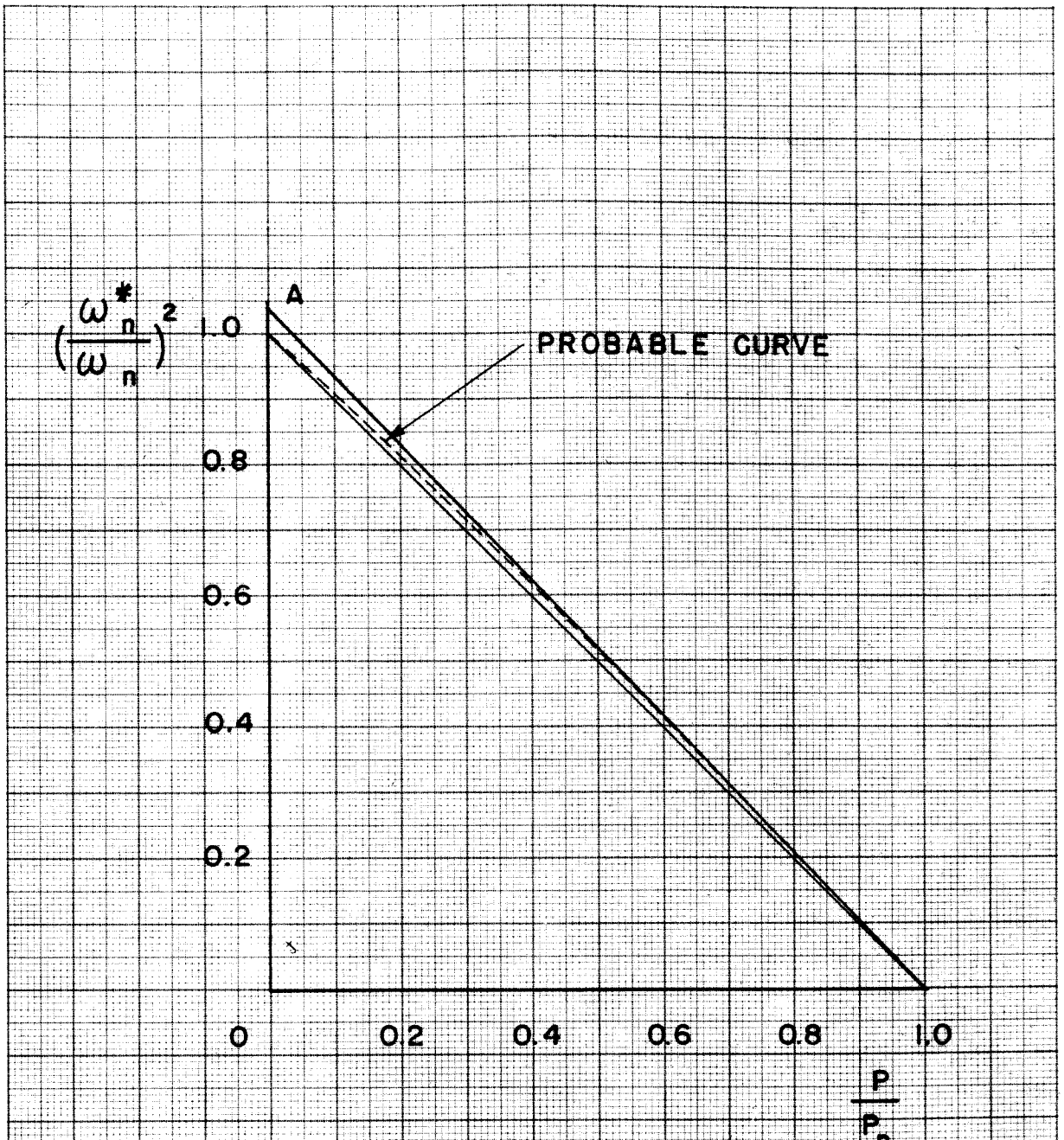

FIG. 2

VARIATION OF FREQUENCY

WITH END LOAD BY ENERGY METHODS

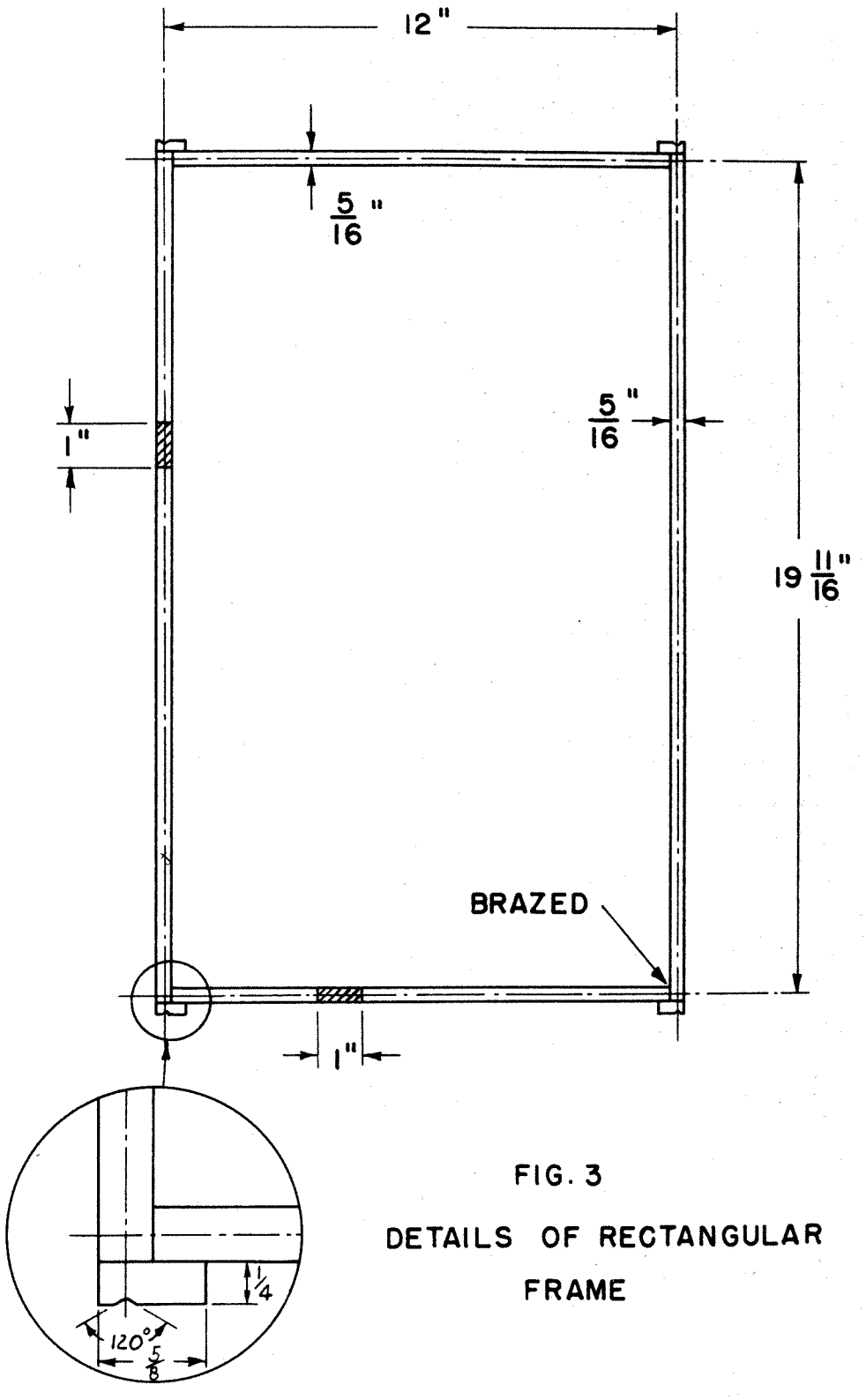

FIG. 3

DETAILS OF RECTANGULAR FRAME

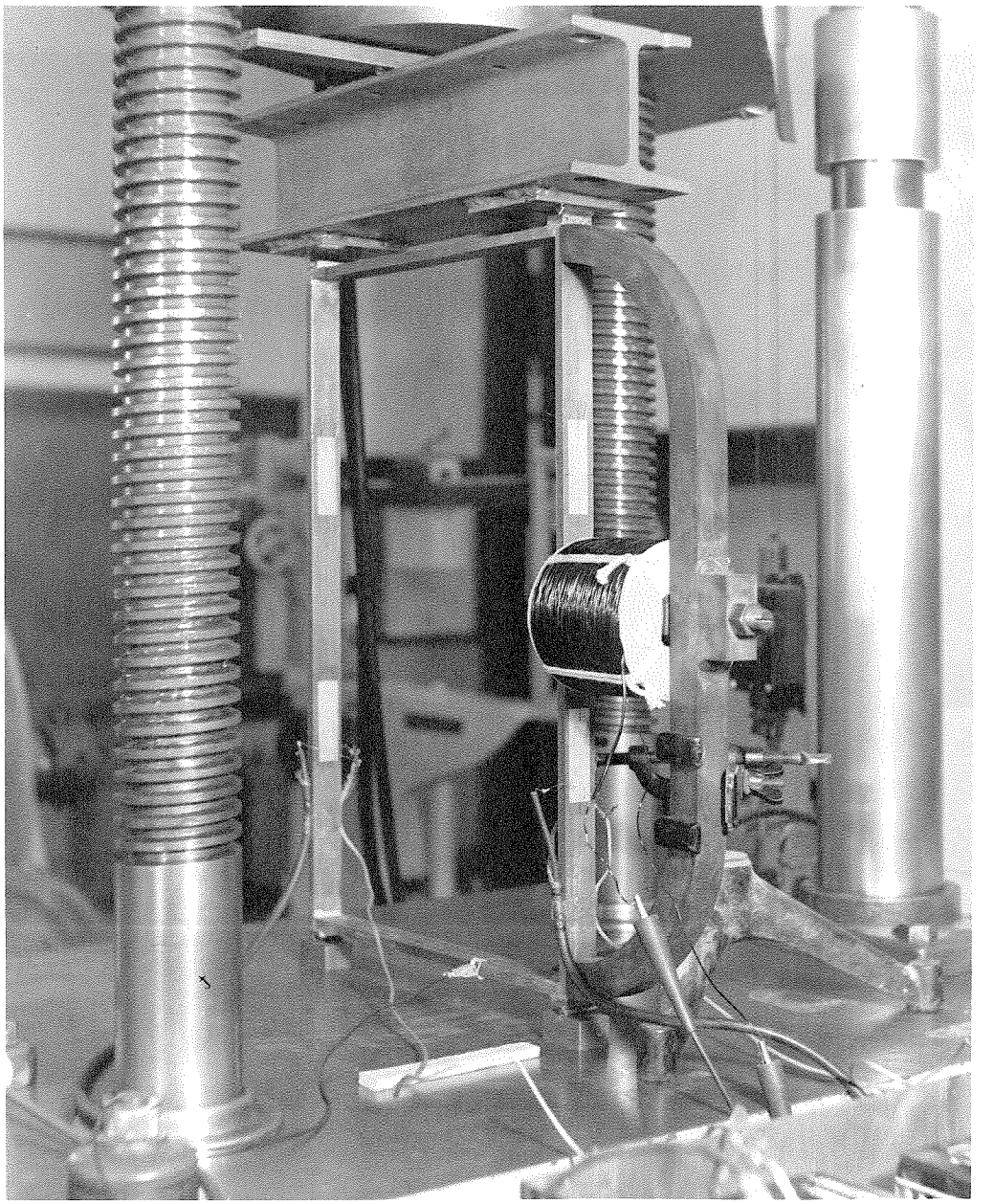

FIG. 4

MAGNETIC OSCILLATOR AND FRAME

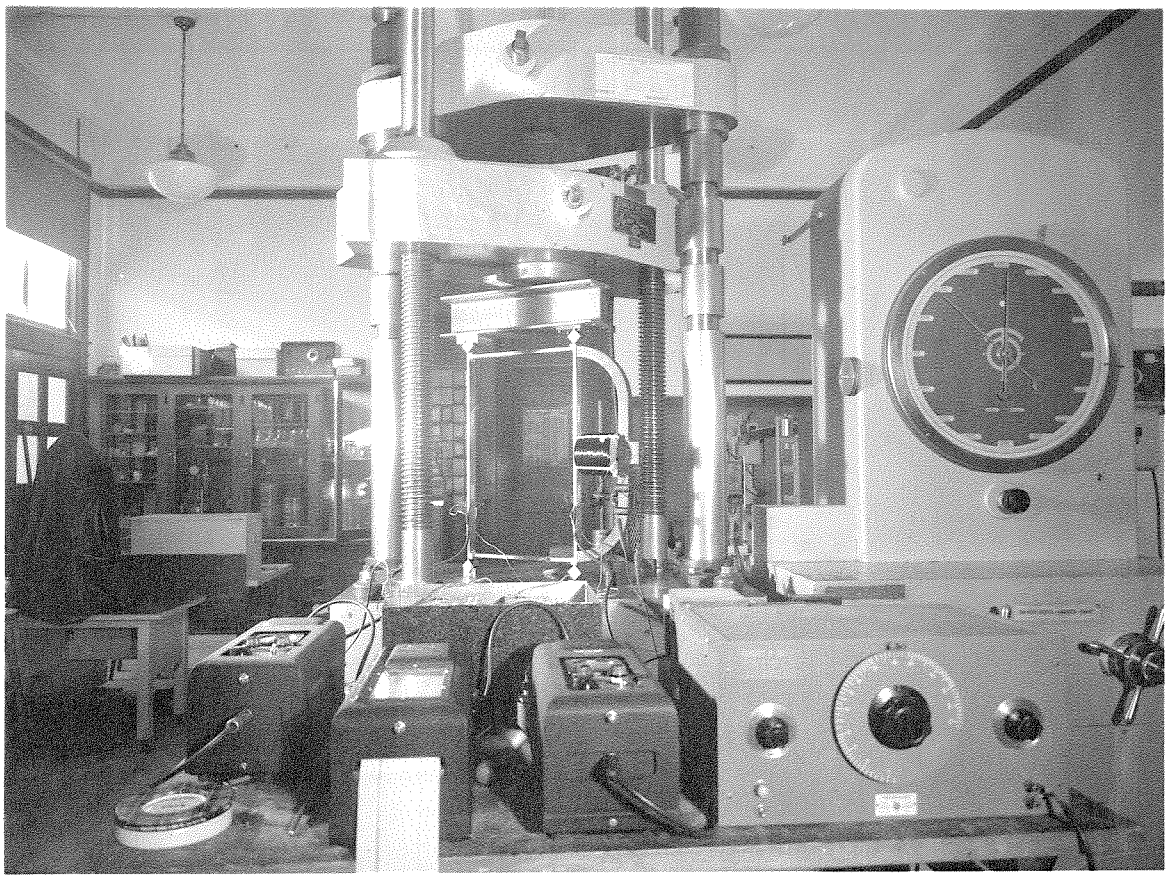

FIG. 5

RECTANGULAR FRAME TEST SET-UP

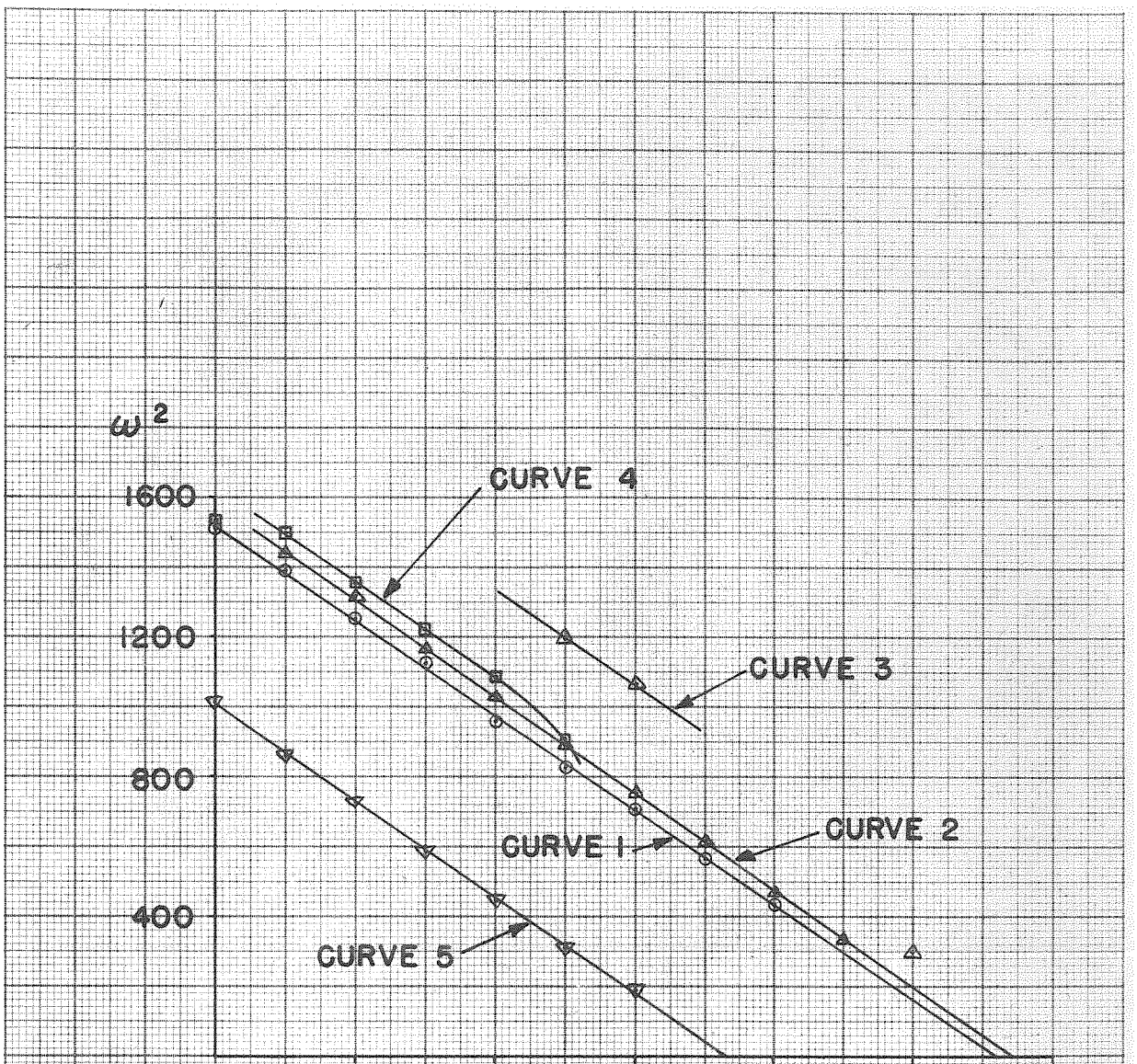

FIG. 6

TEST RESULTS FOR RECTANGULAR FRAME

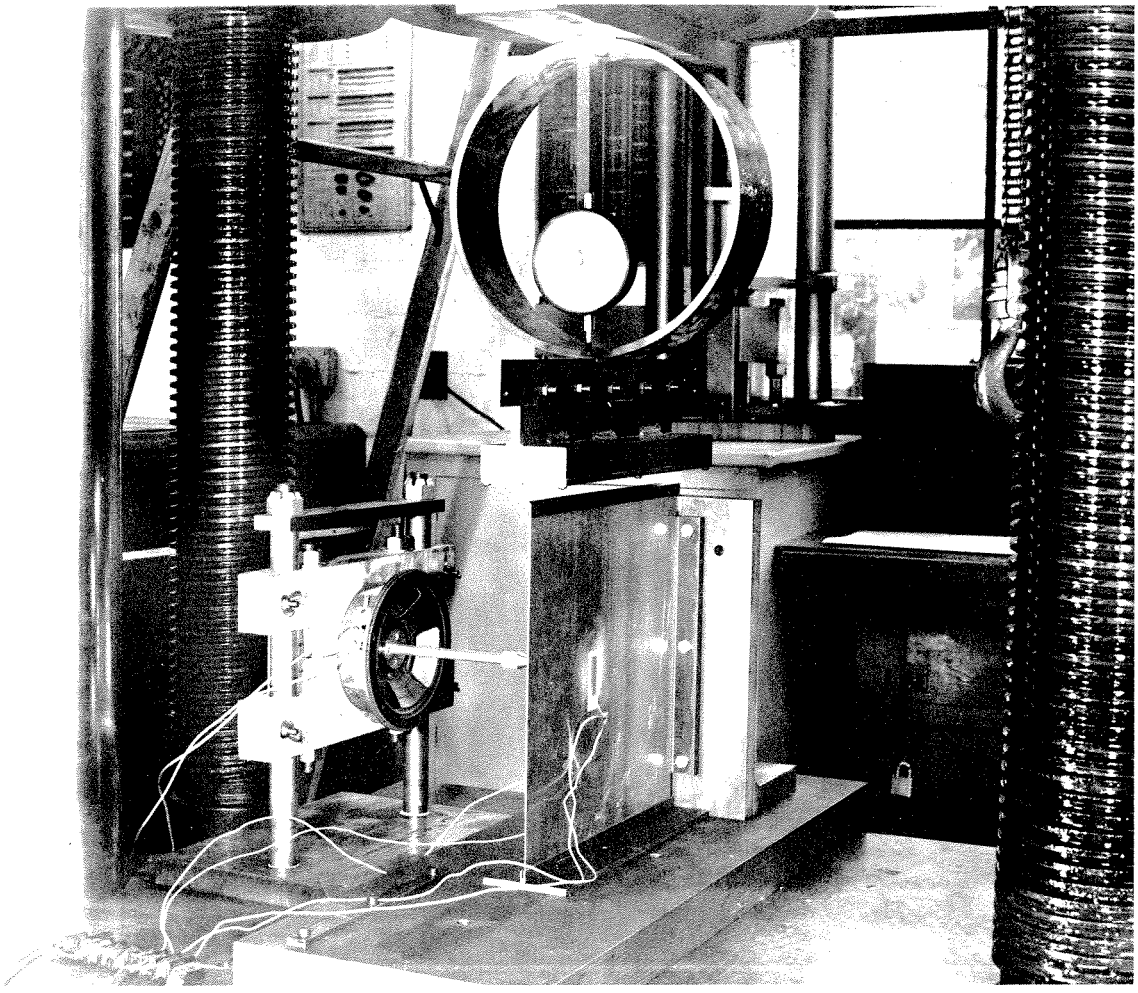

FIG. 7

FLAT PLATE AND OSCILLATOR

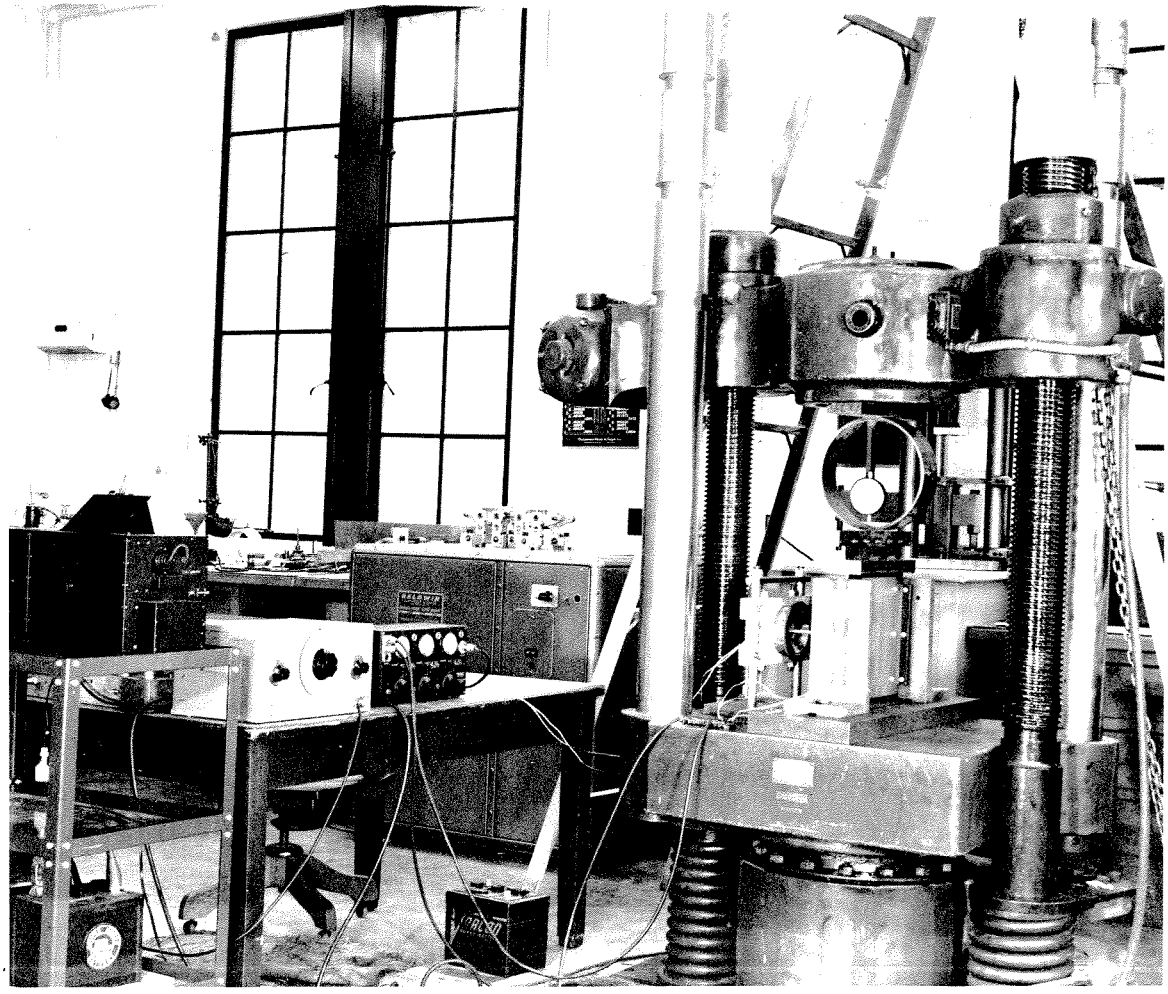

FIG. 8

FLAT PLATE TEST SET-UP

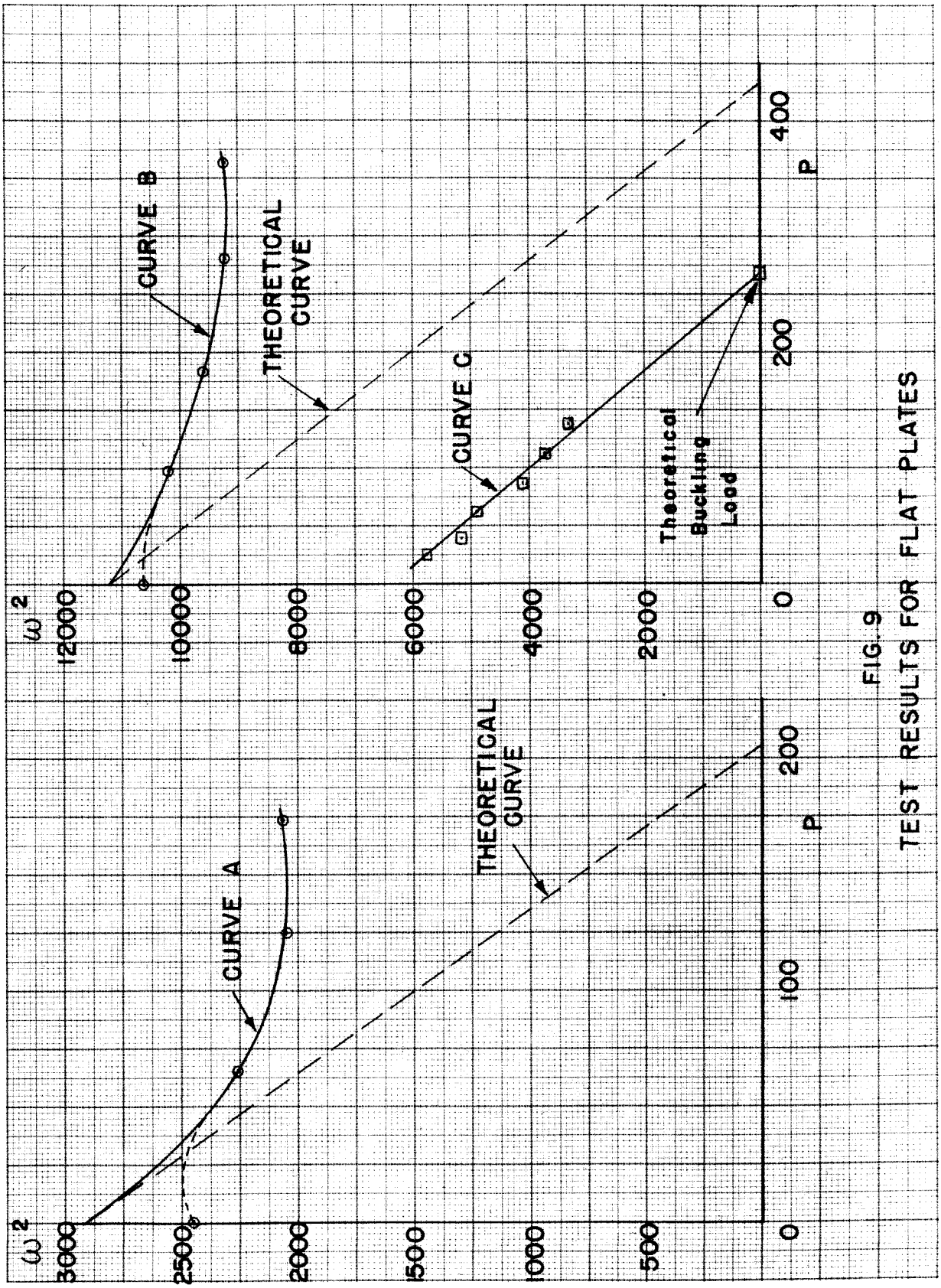

FIG. 9

TEST RESULTS FOR FLAT PLATES

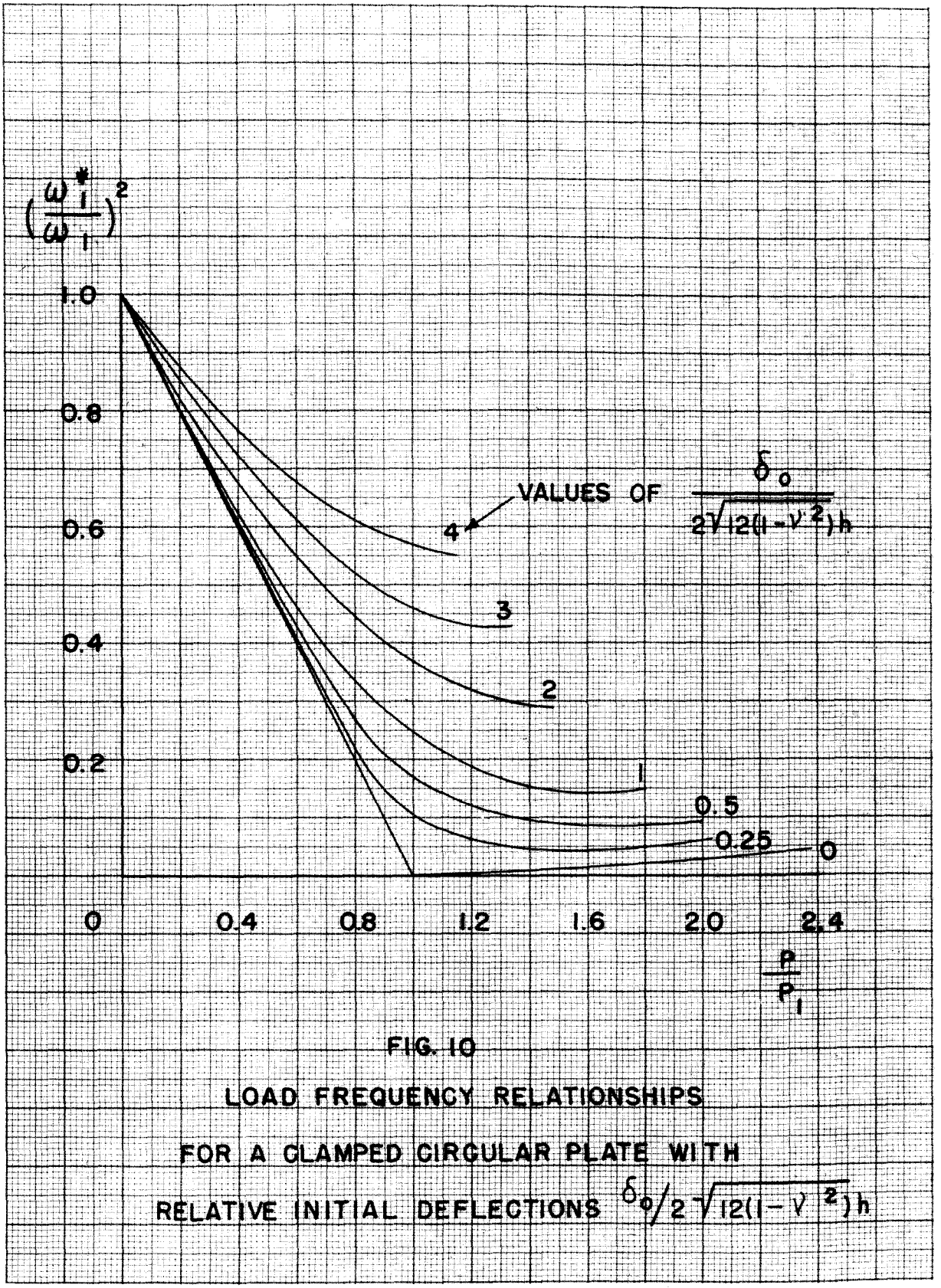

FIG. 10

LOAD FREQUENCY RELATIONSHIPS

FOR A CLAMPED CIRCULAR PLATE WITH

RELATIVE INITIAL DEFLECTIONS $\delta_0/2\sqrt{12(1-\nu^2)}h$

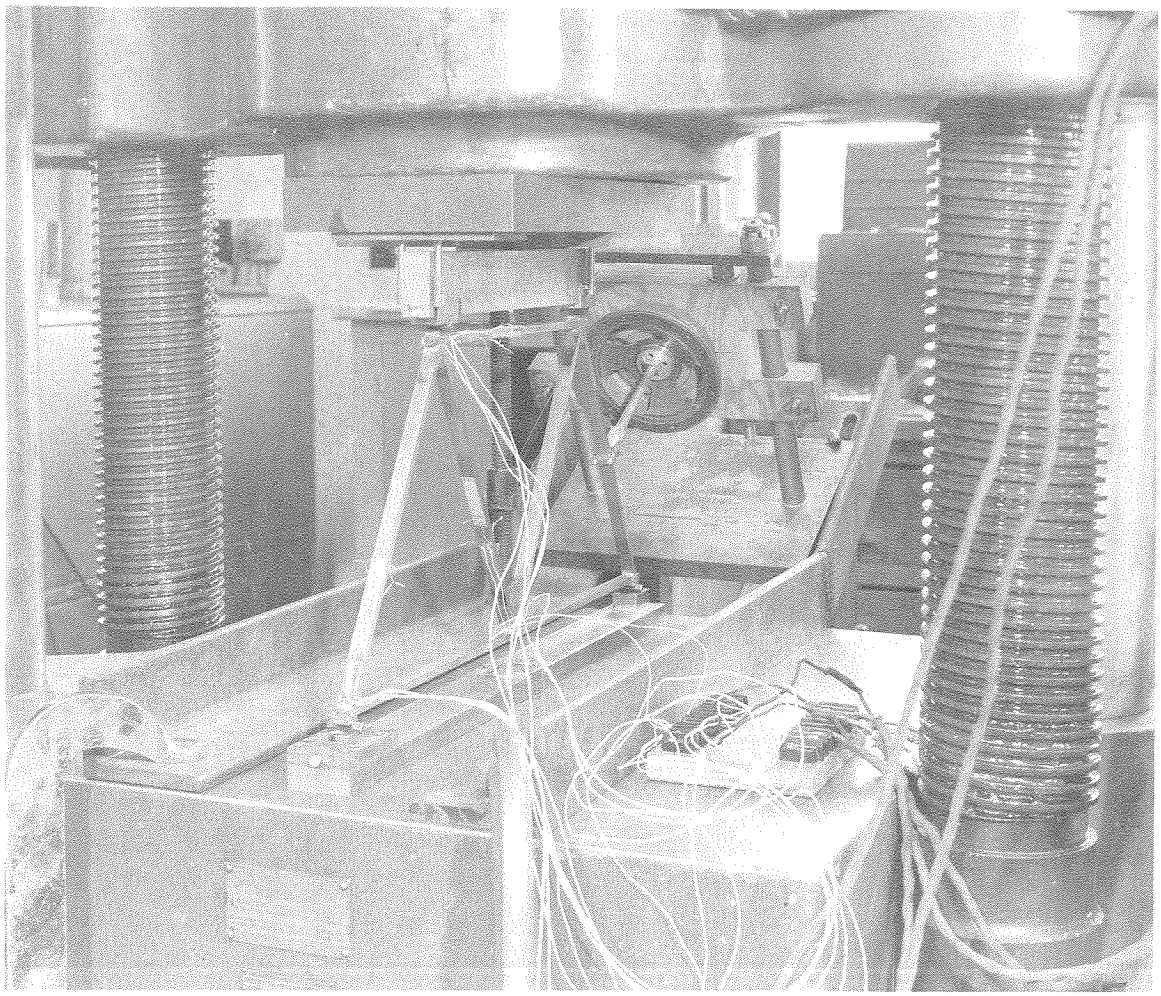

FIG. 11

RIGID TRUSS TEST SET-UP

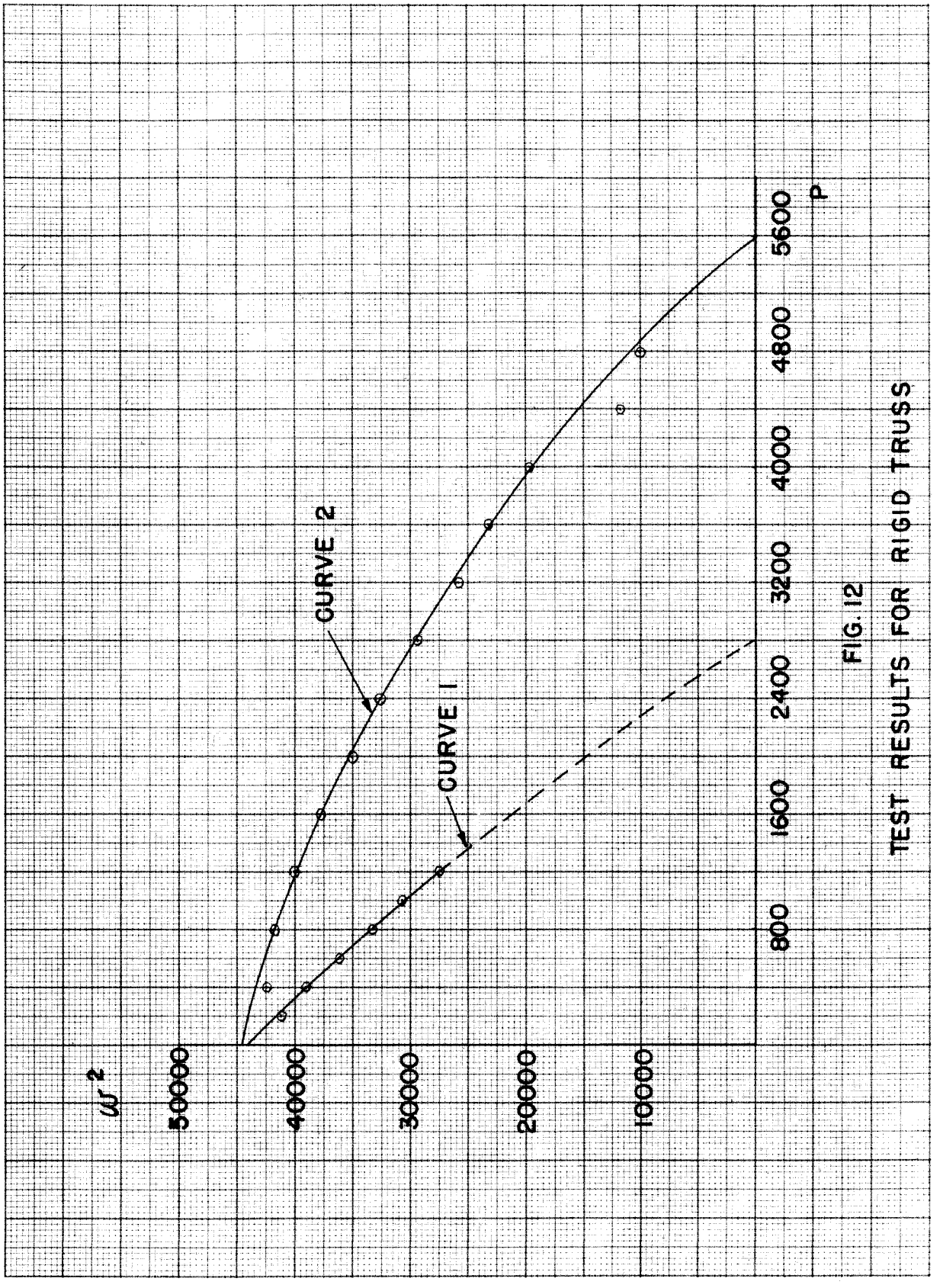

FIG. 12

TEST RESULTS FOR RIGID TRUSS

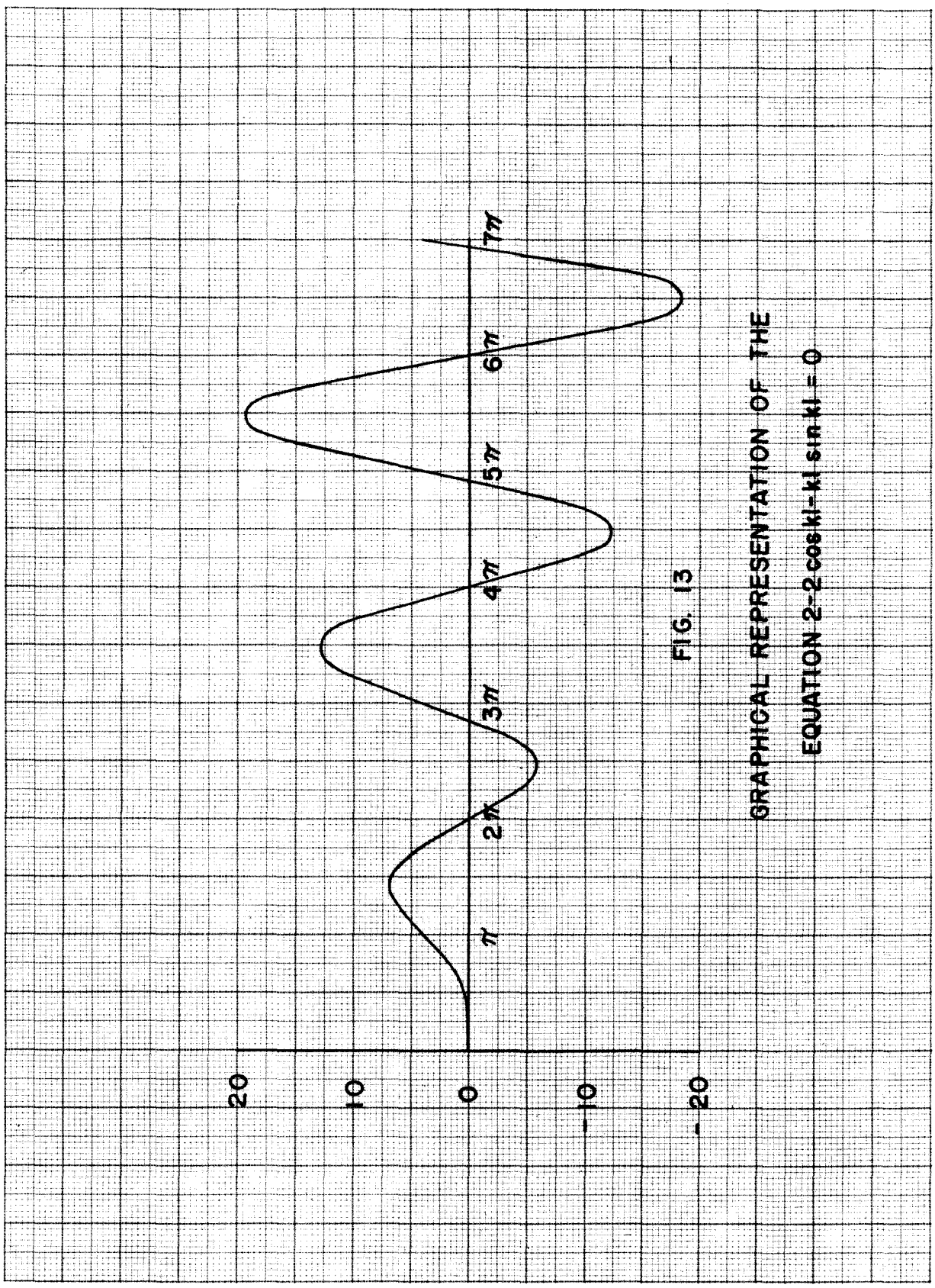

FIG. 13

GRAPHICAL REPRESENTATION OF THE EQUATION $2-2\cos kl-kl\sin kl=0$

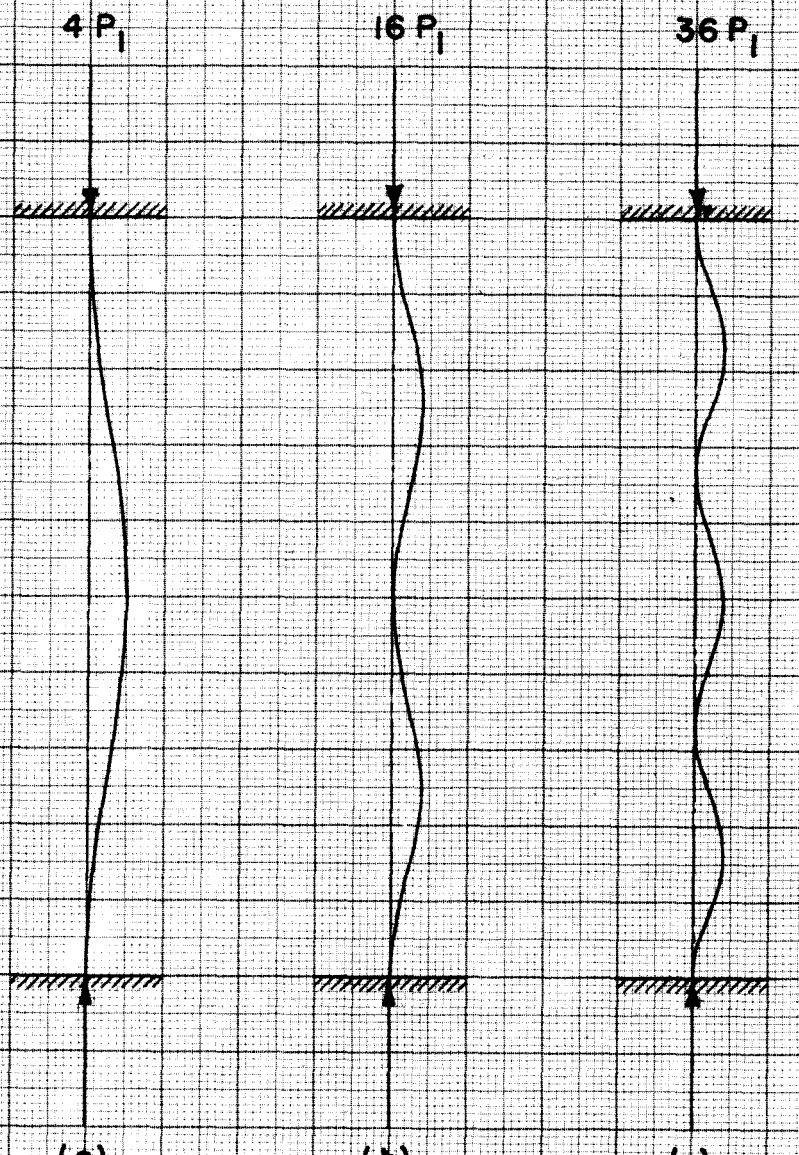

FIG. 14

BUCKLING MODES CORRESPONDING TO THE SOLUTION OF $\sin \frac{kl}{2} = 0$

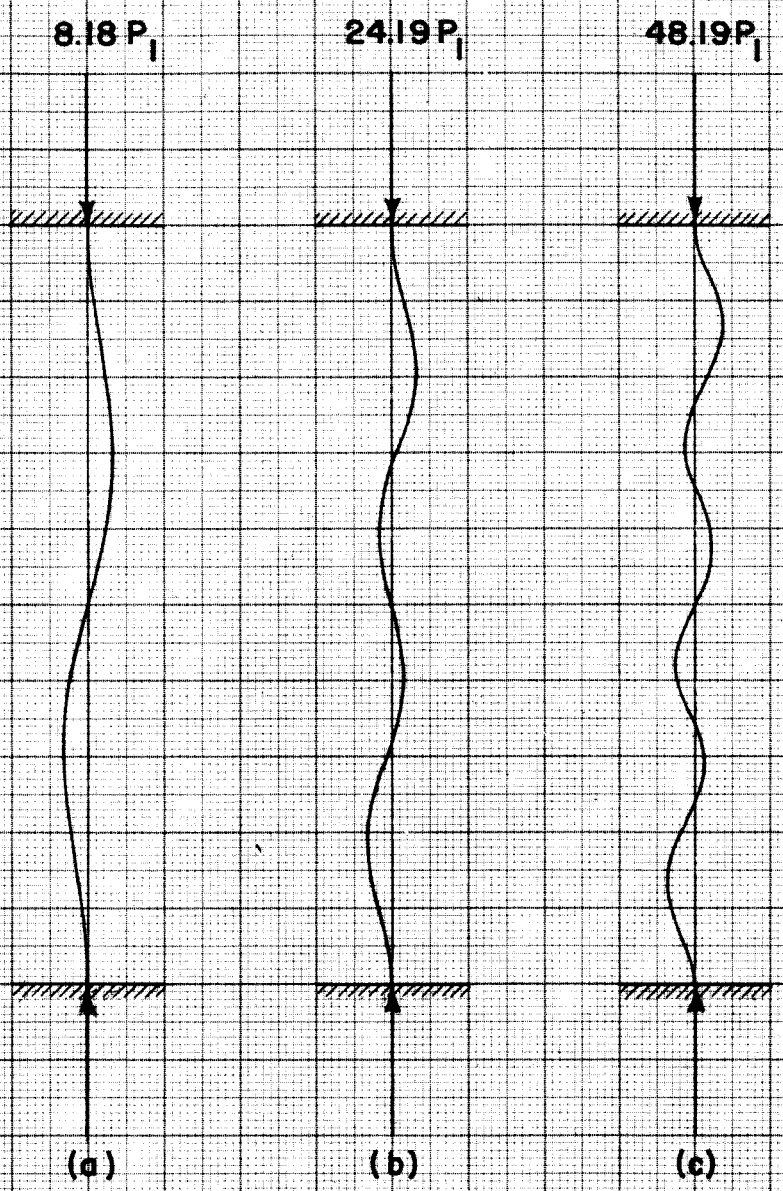

FIG. 15

BUCKLING MODES CORRESPONDING TO THE SOLUTION OF $\tan \frac{kl}{2} = \frac{kl}{2}$

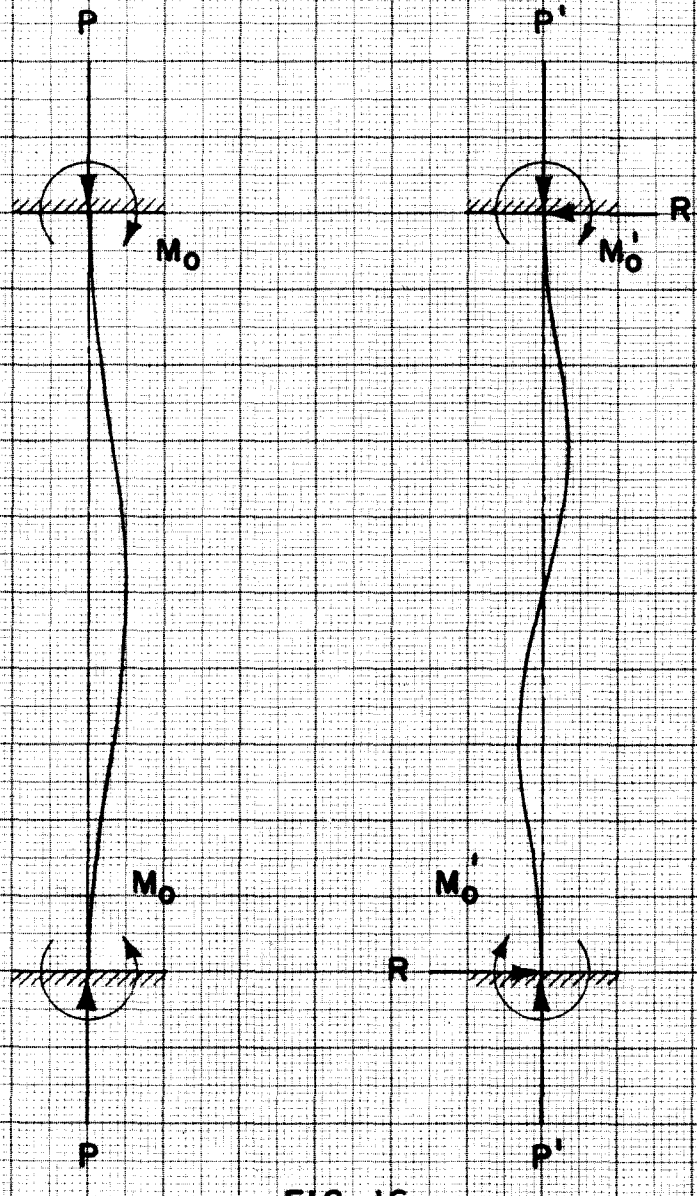

FIG. 16

EXTERNAL FORCES AND MOMENTS
FOR THE TWO TYPES OF BUCKLING